CENTRE d' ETUDES et de RECHERCHES
GEODYNAMIQUES et ASTRONOMIQUES

FIFTH INTERNATIONAL WORKSHOP ON LASER RANGING INSTRUMENTATION

VOLUME II

HERSTMONCEUX CASTLE
SEPTEMBER 10–14 / 1984

PROCEEDINGS
COMPILED AND EDITED BY
J. GAIGNEBET

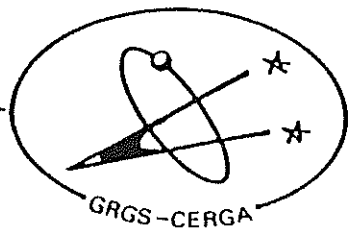

GROUPE de RECHERCHES de GEODESIE SPATIALE

produced by the Geodetic Institute,
University of Bonn, Nussallee 17,
D-5300 Bonn 1
1985

CONTENTS

USE OF THE GLOBAL POSITIONING SYSTEM FOR THE NASA TRANSPORTABLE LASER RANGING NETWORK

C. Wardrip*, P. Kushmeider
Goddard Space Flight Center
Greenbelt, MD 20771 USA

Telephone (301) 344 7000
TWX 710 828 9716

J. Buisson, J. Oaks, M. Lister
Naval Research Laboratory
4555 Overlook avenue S.W. Washington DC 20375

Telephone (202) 545 6700

P. Dachel, T. Stalder
*Bendix Field Engineering Coporation
One Bendix Road
Colombia, Maryland 21045

Telephone (301) 964 7000
Telex 197700

ABSTRACT

Present time synchronization techniques used in the NASA Goddard Space Flight Center (GSFC) Transportable Laser Rangin Network (TLRN) will be discussed. The operational aspects of the Naval Research Laboratory (NRL) developed Global Positioning System (GPS) receiver and the Stanford Telecommunications, Inc. (STI) GPS receiver, both of which are used in the GSFC-TLRN, will also be discussed. In addition, operational time data taken via GPS at TLRN sites located at Goldstone, California ; Santiago, Chile ; Cerra Tollola, Chile ; Otay Mountain, California ; Cabo San Lucas, Mexico and Arequipa, Peru during 1983 and 1984 will be presented.

Use of the Global Positioning System for the NASA Transportable Laser Ranging Network

Introduction

The NASA Goddard Spaceflight Center (GSFC) and the Naval Research Laboratory (NRL) initially transferred time by satellite in 1977 using the NRL Navigation Technology Satellite (NTS) [1,2]. This system provided accuracies of several hundred nanoseconds [3]. As an outgrowth of that program a joint effort was started in 1979 to develop Global Positioning System (GPS) timing receivers using signals radiated by the GPS satellites. These receivers were designed to provide precise time measurements between the time standard of the U.S. Naval Observatory and clocks at remote locations. NASA is currently using the GPS time transfer receivers in the GSFC Transportable Laser Ranging Network (TLRN) in support of the GSFC Crustal Dynamics Program.

Geophysical data suggest that the surface of the earth is composed of rigid plates 50 to 150 kilometers thick. These plates move slowly (1 to 10 centimeters per year) in response to driving forces resulting from motion in the earth's interior.

In 1978 the Crustal Dynamics Project was launched to study the movement of the earth's plates. One of the techniques being used to measure plate motion is Satellite Laser Ranging (SLR). SLR uses the measurement of the time of flight of very short laser pulses to a retroreflector on a satellite [4].

Ground-based lasers transmit intense light pulses to these retroreflectors and record the round-trip travel time for the pulse to return. If the orbit of the satellite is well-known, such ranging permits precise determination of the location of the laser station on the Earth's surface. When two stations range to the same satellite simultaneously, the distance between the stations can be accurately determined.

The GSFC Transportable Laser Ranging Network which supplies the SLR data, presently consists of eight Mobile Laser Systems (MOBLAS, Fig. 1) and four highly Transportable Laser Ranging Systems (TLRS). These systems have been deployed globally to measure regional deformation, plate motion, plate deformation, and polar motion. TLRS-1 and TLRS-2 have been using NRL built GPS receivers since the early part of 1984 and the middle of 1983 respectively. Since the installation of a GPS timing receiver, TLRS-1 (Fig. 2) has gathered data at the following sites: 1) Goldstone, California, USA; 2) Santiago, Chile; and 3) Cerra Tollola, Chile. TLRS-2 (Fig. 3) has obtained GPS time transfer data from: 1) Otay Mountain, California, USA; and 2) Cabo San Lucas, Mexico. Operational GPS time transfer data from these field sites as well as from a semi-permanent laser station in Arequipa, Peru will be presented in this paper.

The NAVSTAR Global Positioning System

NAVSTAR GPS is a tri-service Department of Defense (DOD) program. The first GPS satellite flown was the Navigation Technology Satellite (NTS-II) which was designed and built by NRL personnel [5,6]. GPS provides the capability of very precise instantaneous navigation and transfer of time from any point on the Earth. GPS comprises three segments: The Space Segment, the Control Segment and the User Segment. The phase III Space Segment will consist of a constallation of 18 to 24 satellites, six to eight in

each of three orbital planes (Fig. 4). The satellite orbits are nearly circular at an altitude of about 20,000 km and inclined 55° to the equator. The period is one half of a sideral day, resulting in a constant ground track, but with the satellite appearing 4 minutes earlier each day.

Each satellite transmits its own identification and orbital information continuously. The transmissions are spread spectrum signals, formed by adding the data to a direct sequence code, which is then biphase modulated onto a carrier.

The control segment consists of a master control station (MCS) and monitor stations (MS) placed at various locations around the world [7]. The current Phase I MCS is located at Vandenberg Air Force Base with the support monitor tracking stations at Alaska, Guam, Hawaii, and Vandenberg, California (Fig. 5). The monitor stations collect data from each satellite and transmit to the MCS. The data is processed to determine the orbital characteristics of each satellite and the trajectory information is then uploaded to each satellite, once every 24 hours as the spacecraft passes over the MCS.

The user segment consists of a variety of platforms containing GPS receivers, which track the satellite signals and process the data to determine position and/or time. Navigation is performed by simultaneous or sequential reception of at least four satellites, and time transfer is performed by reception of a single satellite. Coverage of the Phase III constellation is such that at least four satellites will always be in view from any point on the earth's surface.

Time Transfer Method

To transfer time via a GPS satellite, pseudo-range measurements are made consisting of the propagation delay of the received signal biased by the time difference between the satellite clock and the ground station reference clock (see Fig. 6 and references [8] and [9]). Data from the navigation message contain the satellite clock information and the satellite ephemeris, which allows one to compute the satellite position and clock offset. Since the position of the satellite and ground station are known, the propagation delay can be computed, subtracted from the pseudo-range and then corrected for the GPS time offset to determine the results of ground station time relative to GPS time. The navigation message also contains coefficients which allow GPS time to be referenced to the U.S. Naval Observatory (USNO) time standard, therefore, the final result of ground station time relative to USNO time can be calculated in real time. The final results obtained from a single frequency receiver will contain a small error

due to the atmospheric delay, which may be modeled and corrected. If two ground station clocks are synchronized to GPS time, the results can be subtracted to obtain the time difference between the ground station clocks. This can be done at any time, but the best results are obtained when data is taken simultaneously by each ground station from the same satellite (common view), since any error contributed by the satellite is reduced when the data is subtracted.

GPS Time Transfer Receiver (TTR)

The GPS TTR [8] is a microcomputer based system which operates at the single L-band frequency of 1575 MHz (Fig. 7). The receiver uses the C/A code only (1.023 MHz), tracking this code to within 3% of a chip (30 ns). The receiver has the capability to track satellites throughout their doppler range from horizon to horizon, and can track any GPS satellite by changing the receiver internal code. The block diagram in Fig. 8 shows the GPS receiver configuration. Operator interface with the receiver is provided by a keyboard and CRT display. The time data is stored on floppy disks and can also be outputted to an external printer or computer via a serial data interface. The input requirements to the receiver include the antenna position in WGS-72 coordinates, 1 pulse per second from the station time standard and 5 MHz from the station time standard.

Method of Measurement

The NRL built GPS time transfer receivers are currently being operated in MOBLAS 1 and 5, TLRS 1 and 2, and a semi-permanent laser site in Arequipa, Peru. The timing receiver interfaces with the laser system as shown in Fig. 9. Figure 10 contains a block diagram of the TLRS timing subsystem. The TLRS systems require a minimum of 200 minutes of useable laser measurements at a given site before relocation to a new installation. The one pulse per second and 5 MHz input signals required by the receiver are supplied by the station cesium beam clock. The receiver operates in a fully automatic schedule mode, tracking each GPS satellite once per day. The tracking schedule is determined by the operator. Each satellite track is usually scheduled to last ten minutes. Two minutes are required for signal search and acquisition, and one minute for locking and synchronizing to the satellite data. The time transfer results of (Station - USNO) and (Station - GPS) are then sent to the Precise Timing Section of Bendix Field Engineering Corporation (BFEC) in Columbia, Maryland, USA for further processing.

GPS Time Transfer Results

The first TLRS-1 site visited with a GPS timing receiver was Goldstone, California (GDS). Figure 11 shows the time transfer results of the GDS station clock relative to the United States Naval Observatory clock ensemble (denoted by NOB in all of the data plots). The time transfer in microseconds is plotted by days. The term "predicted" indicates that these results were obtained directly from the spacecraft. Figure 12 contains the same time transfer results, namely, (NOB-GDS), however these values are calculated by differencing the (GDS-GPS) data received using the NRL receiver and (NOB-GPS) data obtained via a similar receiver at USNO. The plots of this common view method of time transfer are labeled "observed". Both the predicted and observed plots have a statistical summary included. This summary contains a time transfer in microseconds, a frequency offset term in parts in 10^{13}, an aging term in parts in 10^{14} per day, the root mean square (RMS) fit in nanoseconds, the number of points used and the number of points filtered for each satellite. The satellites are identified by NAVSTAR numbers. There is also a composite line which incorporates the data from all satellites. The time transfer, frequency and aging terms are all calculated for the epoch day shown above the summary table. Because the TLRN sites all use cesium beam clocks a first degree curve is fit to the data, therefore there is no aging term. While the RMS values of the individual satellites are all within the TLRN system requirements of 100 ns, the observed data appears to be noisier then the predicted data. Generally, the common view technique of time transfer yields more accurate results than using the predicted USNO term from the space vehicle. However, common view assumes that two stations track the same GPS satellite at the same time, and this was not the case at the GDS station. The tracking schedule used at GDS differed from the USNO schedule by as much as 12 hours. Therefore, the results shown in the observed plot are less precise.

After the GDS site the TLRS-1 system was relocated to Santiago, Chile (denoted by AGO in the data plots). Figures 13 and 14 show the predicted and observed time transfer results of AGO relative to USNO, (NOB-AGO), for the entire period of time the station was in operation. Several discontinuities are obvious on these plots. The first discontinuity, occurring on day 78, was due to a discrete jump in the station cesium of approximately 10 microseconds. The second obvious discontinuity is the result of a new station cesium clock being installed. The original cesium failed on day 93 and the new cesium began operation on day 98. Two other less obvious discontinuities can be found on the predicted plot but do not show up in the observed data. These jumps, occurring on days 84 and 105, are the results

of accumulated error in the predicted USNO term. The USNO prediction is transmitted by each GPS satellite, as part of the navigation message, once every 12.5 minutes. The NRL receiver does not update the USNO prediction for each satellite track due to the length of time this would require. Rather, a special track is used by the receiver to update the entire navigation message, including the USNO term. This track, scheduled once a day and lasting 20 minutes, can be taken from a GPS satellite. If the predicted USNO term is not updated daily, the error will grow rapidly. Errors on the order of several hundred nanoseconds have been observed when the USNO prediction is a few days old. This error does not exist when the common view technique is used between a remote station and USNO. The observed plot of (NOB-AGO), (Fig. 14), therefore contains no discontinuities on days 84 and 105.

The Santiago station data has been subdivided into its three distinct phases and the predicted and observed data for each phase is shown plotted in Figs. 15 through 20. In each of these plots there is an obvious bias in the data from one satellite to another. This problem results when the coordinates of the receiver's antenna are inaccurate. The best time transfer results are obtained when the position of the antenna is known to within 3 meters. The observed plots reveal that these results are consistently superior to the predicted method. However, it should be noted that the predicted results are within the requirements of the TLRN system.

From Santiago the TLRS-1 system was moved to Cerra Tollola, Chile (TOL). The entire data set, both predicted and observed, can be found in Figs. 21 and 22. These graphs indicate that there was an antenna coordinate error upon system installation. On day 145 new coordinates were determined and input to the GPS receiver. The predicted and observed data after this coordinate change have been plotted and are shown in Fig. 23 and 24. Again, both the predicted and observed results are within TLRN system requirements, with the observed data having a slightly lower RMS.

In the later part of 1983 the TLRS-2 systems was deployed with a GPS receiver at Otay Mountain, California (OTY). TLRS-2 remained at this location for over 100 days and gathered much data (Figs. 25 and 26). All discontinuities on these graphs are the result of phase adjustments to the station cesium clock. Station personnel were required to keep the TLRS-2 clock synchronized with USNO time to within a few microseconds. Figures 27 and 28 show a representative sample of predicted and observed data from the Mt. Otay site. This sample covers the period from day

271 through day 284 in 1983. Again a lower RMS can be seen in the observed data, with the predicted data fulfilling system requirements.

The next site TLRS-2 visited was Cabo San Lucas, Mexico (CSL). The predicted and observed plots are shown in Figs. 29 and 30 respectively. Only NAVSTAR 4 appears in the statistical summary of the observed plot because the program that generates these plots requires five tracks of a particular satellite in order to calculate the summary information. The satellite tracking schedule used at CSL differed somewhat from that used at USNO, therefore the number of common view points on the observed plot is lower than the total number of points on the predicted plot.

The final laser site to be discussed is a semi-permanent station in Arequipa, Peru (ARP) which supports the NASA GSFC Crustal Dynamics Program. A GPS receiver was installed at this location in the first quarter of 1984 (Fig. 31). The predicted and observed graphs are shown in Figs. 32 and 33. The discontinuities on the predicted plot occurring on days 107 and 118 are due to accumulated error in the predicted USNO term due to lack of update. These discontinuites, therefore, do not appear on the observed plot. Other discontinuities are the results of phase adjustments to the station cesium clock. Figures 34 and 35 contain the predicted and observed graphs for the period between days 125 and 167. Again, because of the difference in satellite tracking schedules between ARP and USNO, an ideal common view situation does not exist. Therefore, the predicted and observed results show little difference.

Future TLRN Systems

NRL built GPS time transfer receivers were recently installed in MOBLAS-1 deployed at Huahine, French Polynesia and MOBLAS-5 at Yarragadie, Australia. GPS time transfer data from these stations was not available at this writing.

The TLRS 3 and 4 systems are currently under development and testing at the NASA Goddard Space Flight Center. These TLRS systems will be using GPS timing receivers manufactured by Stanford Telecommunications, Inc. (STI). The STI receivers have been procured and are currently being tested at GSFC. Experimental data obtained under laboratory conditions at the GSFC laser laboratory using the STI receivers is shown in Fig. 36. The receivers were operated using an internal rubidium oscillator included in the STI receivers as an option. Therefore, a second degree curve has been fit to this data which results in an aging term being calculated and included in the summaries of Fig. 36. The STI receiver outputs the station time difference relative to either USNO or GPS, but not

both simultaneously. In these experiments the receivers were operated with the time difference relative to USNO, therefore, only the predicted plot can be shown.

Conclusion

The results of the operational data, gathered by the NRL built GPS time transfer receivers at field sites, indicate that the overall accuracy of the synchronization via the Global Positioning System is consistently better than 100 nanoseconds, which meets the synchronization requirement of the NASA laser ranging network. The results of the experimental data gathered by the STI timing receivers under laboratory conditions indicate that these receivers will also meet the TLRN system synchronization requirements. Field tests on the STI receivers are scheduled for the near future.

References

1. L. Raymond, O. J. Oaks, J. Osbone, G. Whitworth, J. Buisson, P. Landis, C. Wardrip, and J. Perry, "Navigation Technology Satellite (NTS) Low Cost Timing Receiver," Goddard Space Flight Center Report X814-77-205, Aug. 1977.

2. O. J. Oaks, Jr., J. A. Buisson, and T. B. McCaskill, "Initial Design for NTS Time Transfer Receiver," NRL Report 8312, May 1979.

3. J. Buisson, T. McCaskill, J. Oaks, D. Lynch, C. Wardrip, and G. Whitworth, "Submicrosecond Comparisons of Time Standards via the Navigation Technology Satellites (NTS)," pp. 601-627 in Proceedings of the Tenth Annual Precise Time and Time Interval (PTTI) Applications and Planning Meeting, Nov. 1978, NASA Technical Memorandum 80250.

4. "Laser Stations - Plant Facilities Development and Station Description," Goddard Space Flight Center Report MF-176, August 1983.

5. R. L. Easton, J. A. Buisson, and T. B. McCaskill, "Initial Results of the NAVSTAR GPS NTS-2 Satellite," NRL Report 8232, May 1978.

6. R. L. Easton, J. A. Buisson, T. B. McCaskill, O. J. Oaks, S. Stebbins, and M. Jeffries, "The Contribution of Navigation Technology Satellites to the Global Positioning System," NRL Report 8360, Dec. 1979.

7. S. S. Russell and J. H. Schaibly, "Control Segment and User Performance," Navigation (J. Inst. Navigation) 25(2), 166-172 (1978).

8. J. Oaks, J. Buisson, C. Wardrip - "GPS Time Transfer Receivers for the NASA Transportable Laser Ranging Network", NASA/GSFC x-814-82-6, April 1982.

9. J. Oaks, A. Frank, S. Falvey, M. Lister, J. Buisson, S. Wardrip and H. Warren, "Prototype Design and Initial Test Evaluation of a GPS Time Transfer Receiver", NRL report 8608, July 27, 1982.

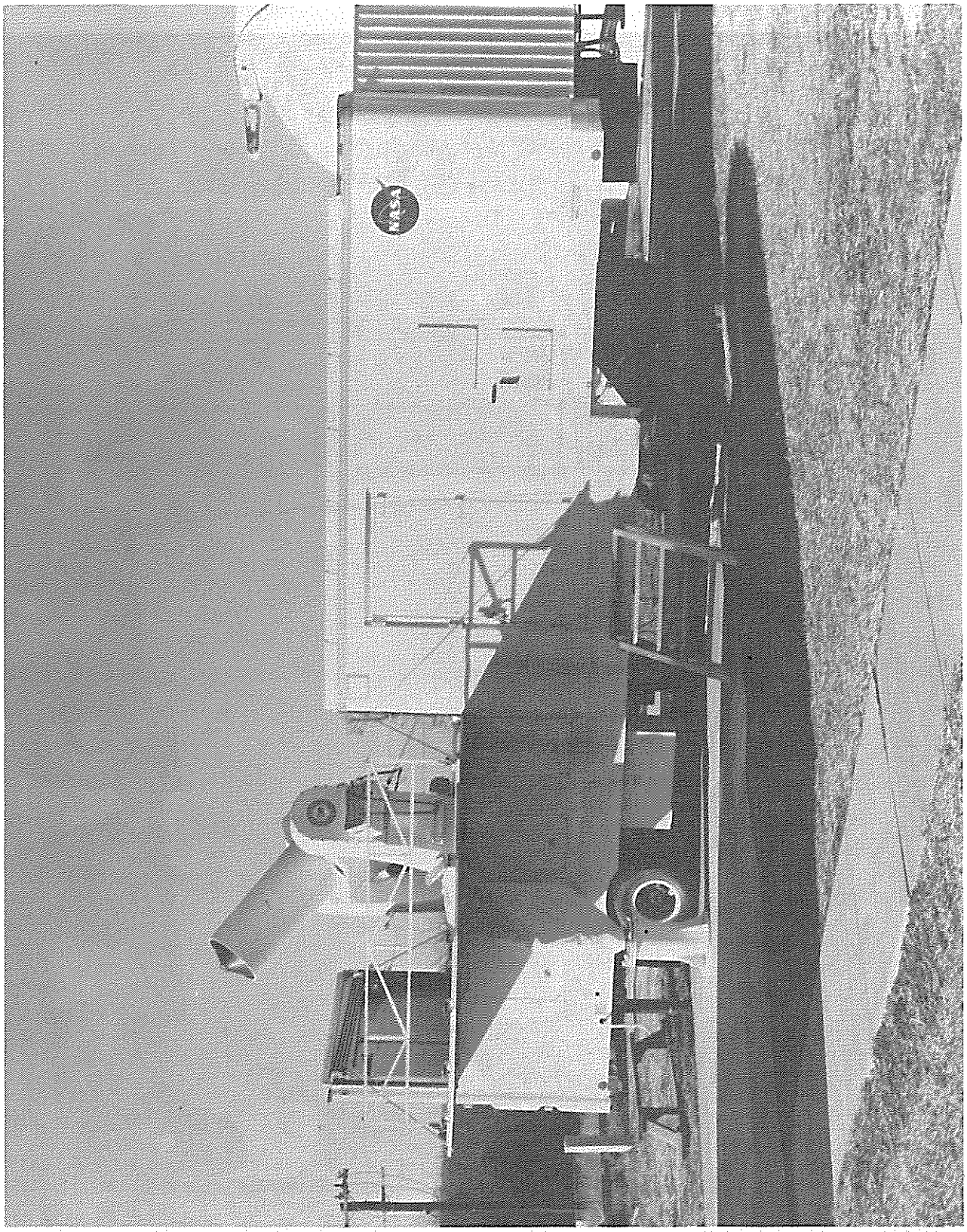

Figure 1 Mobile Laser System (MOBILAS) Van.

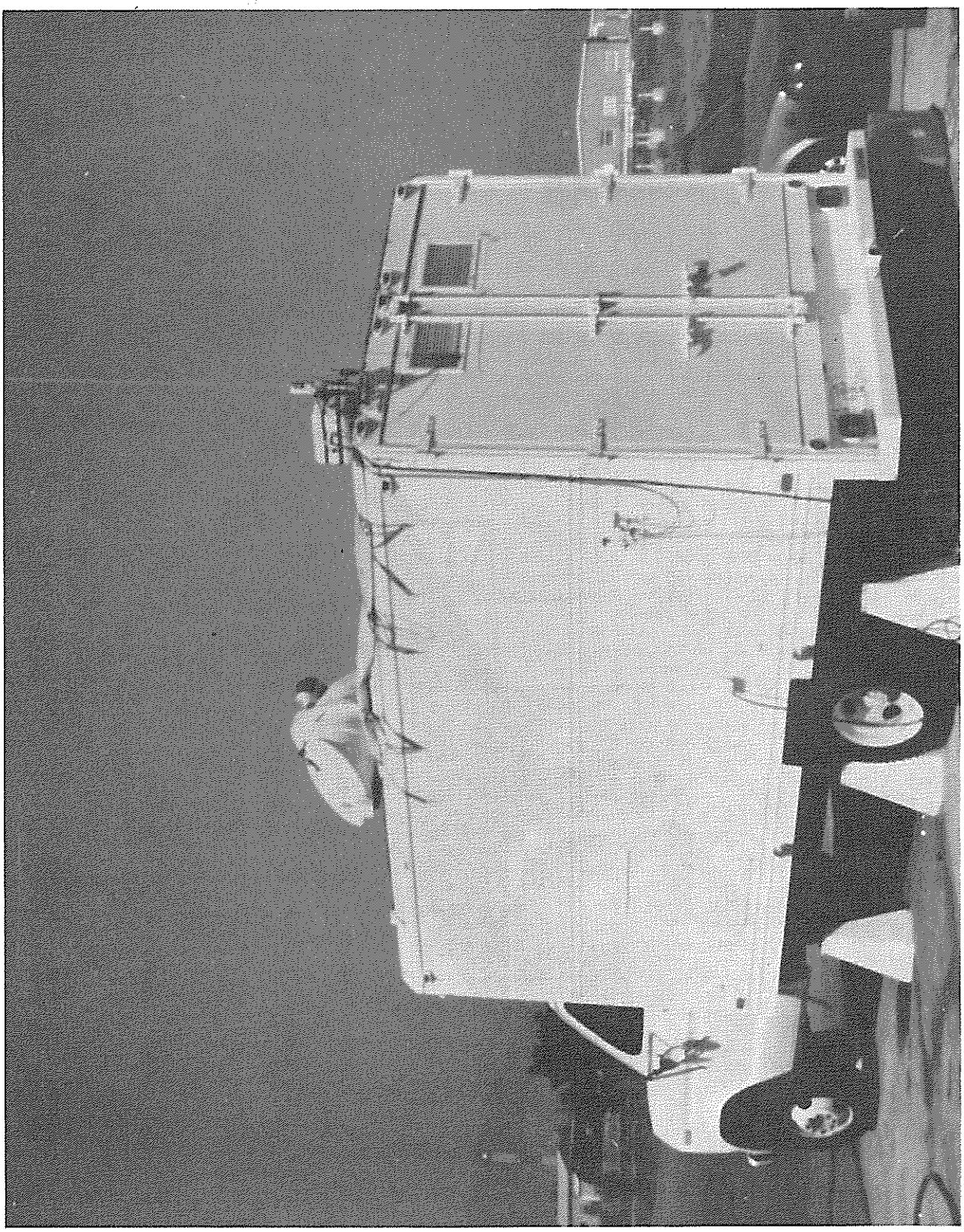

Figure 2 Transportable Laser System (TLRS-1) Van.

Figure 3 Transportable Laser System (TLRS-2) Dome.

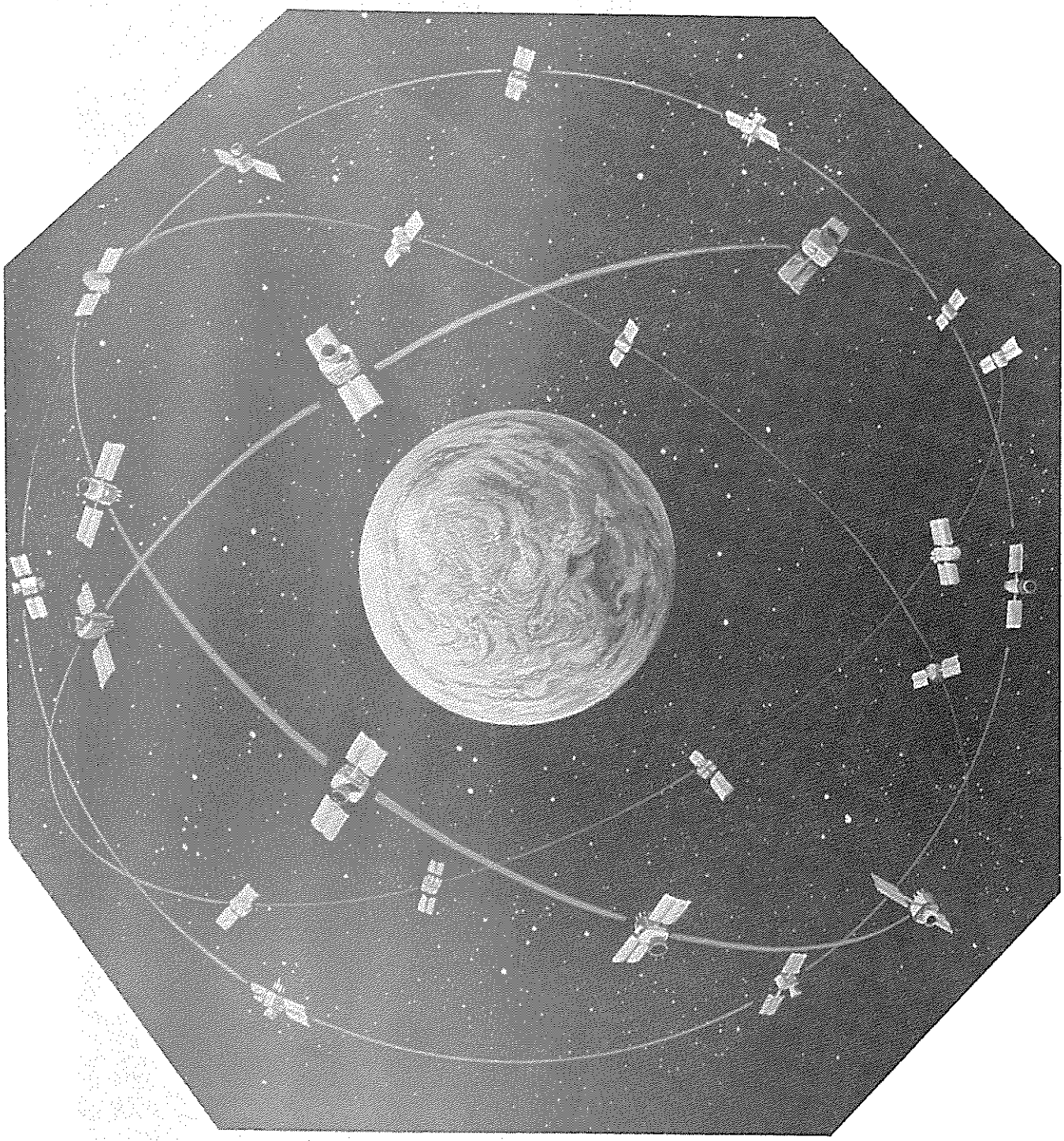

Figure 4 The NAVSTAR Global Positioning System.

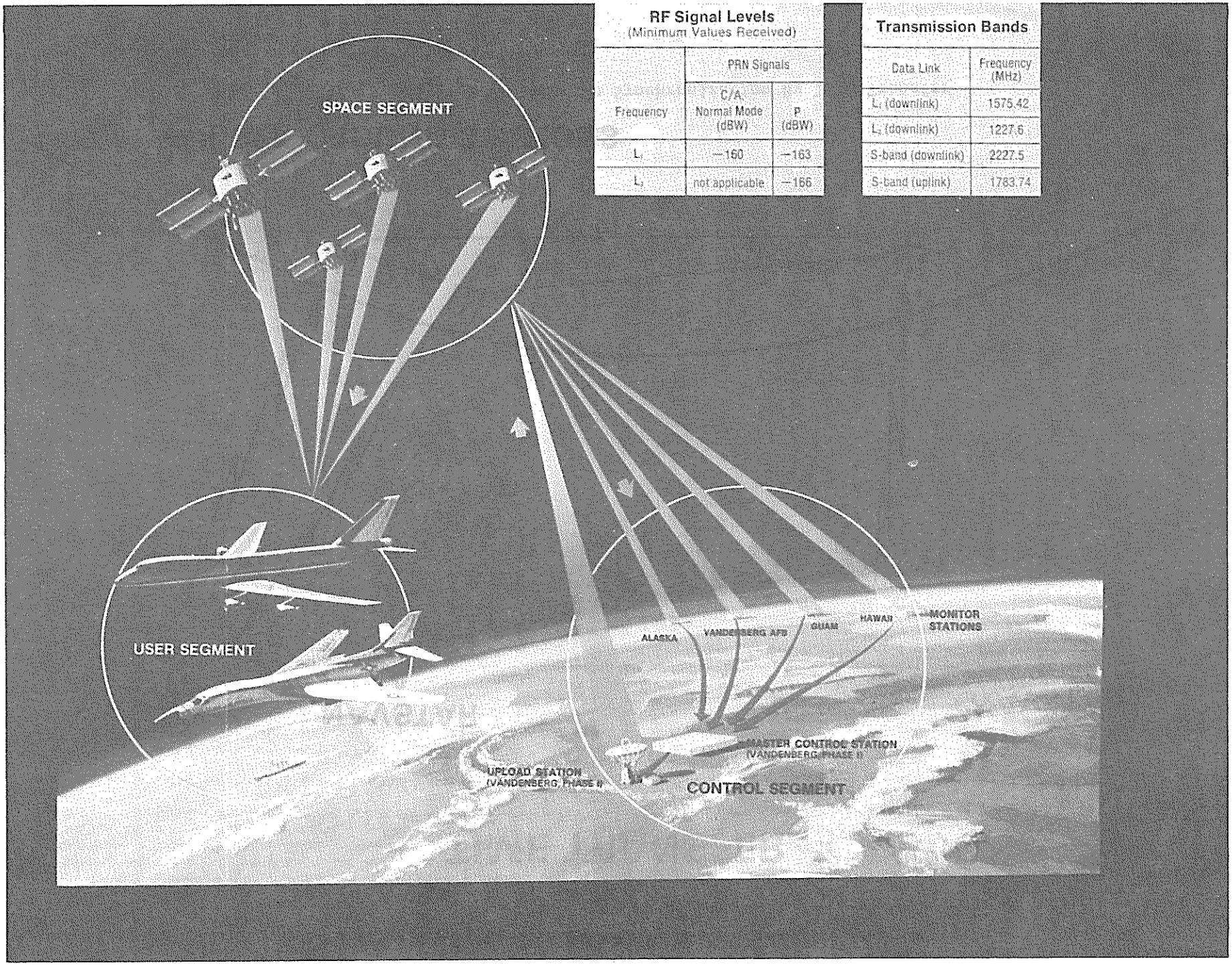

RF Signal Levels
(Minimum Values Received)

Frequency	PRN Signals	
	C/A Normal Mode (dBW)	P (dBW)
L_1	−160	−163
L_2	not applicable	−166

Transmission Bands

Data Link	Frequency (MHz)
L_1 (downlink)	1575.42
L_2 (downlink)	1227.6
S-band (downlink)	2227.5
S-band (uplink)	1783.74

Figure 5 NAVSTAR Global Positioning System Segments.

NAVSTAR GPS
STATION SYNCHRONIZATION
BY
TIME TRANSFER

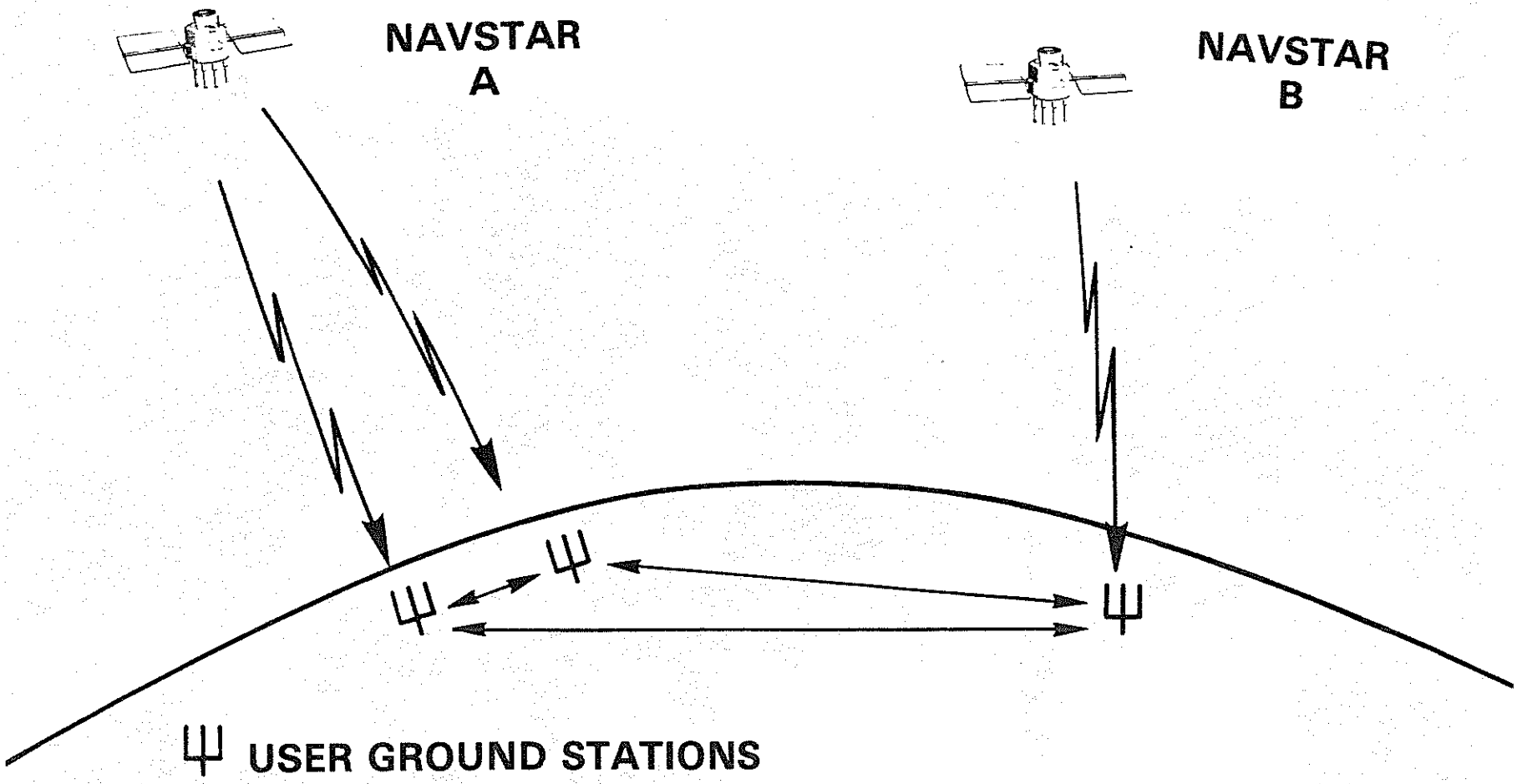

Fig. 6 NAVSTAR GPS Station Synchronization By Time Transfer

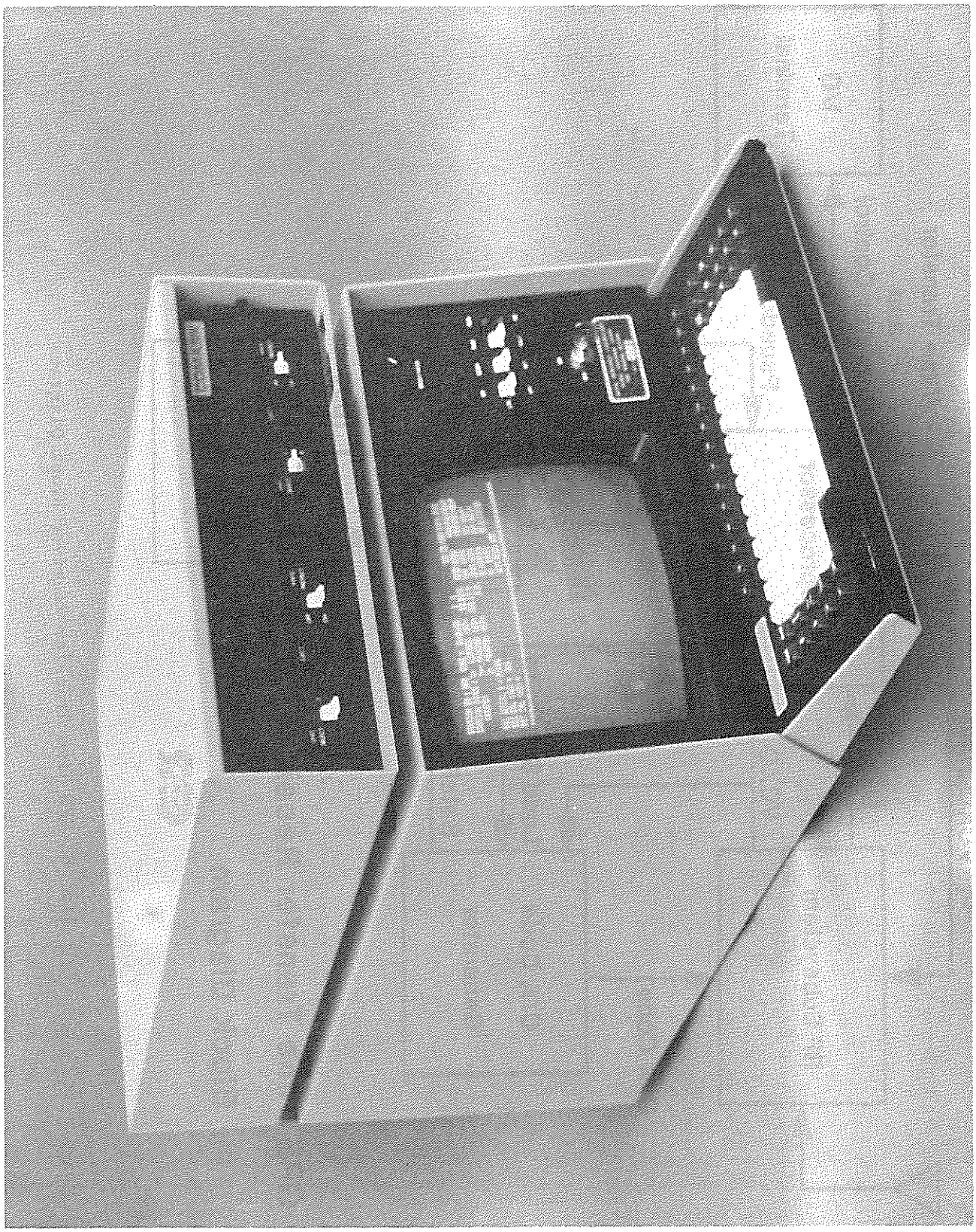

Figure 7 Naval Research Laboratory GPS Receiver.

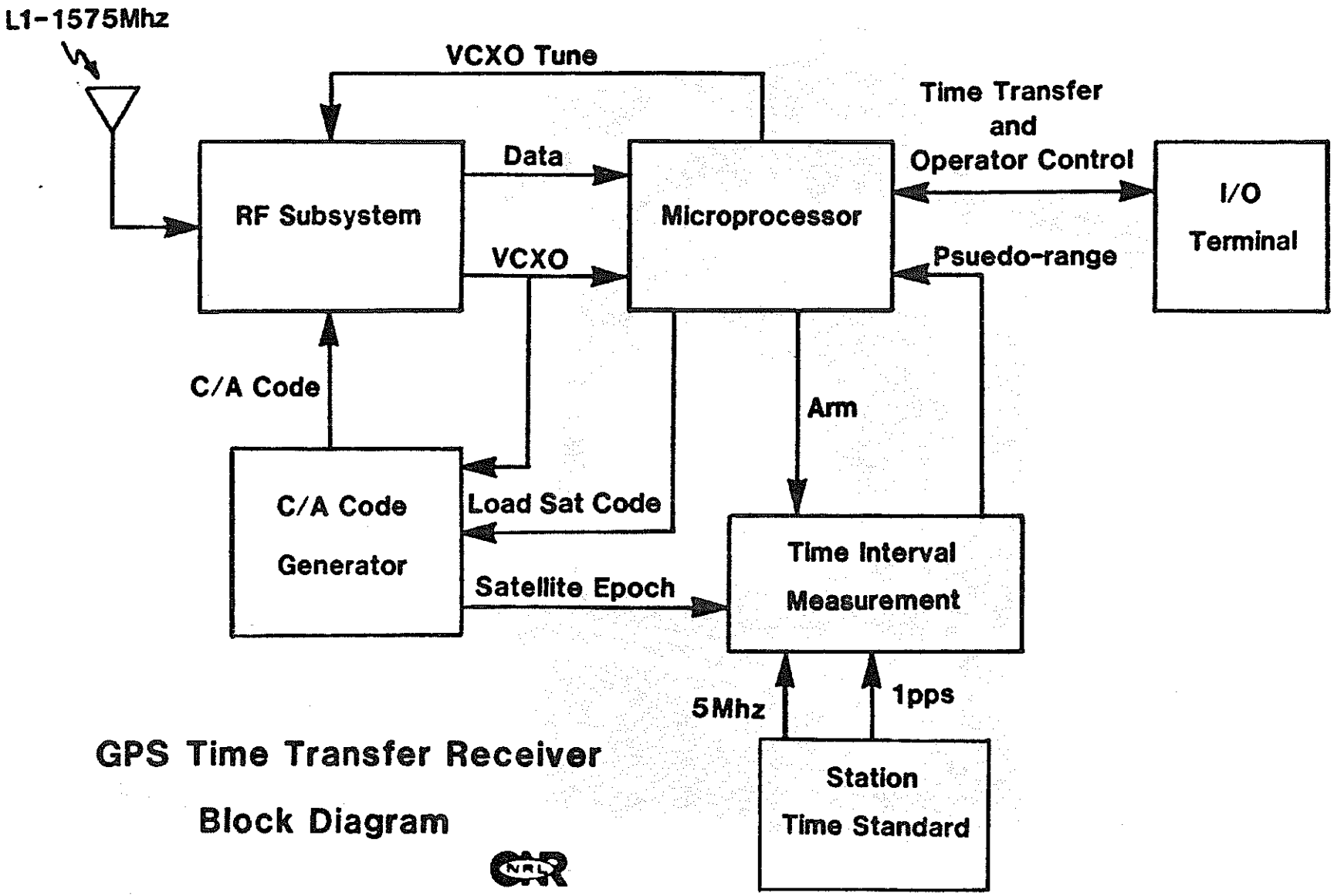

Fig. 8 GPS Time Transfer Receiver Block Diagram

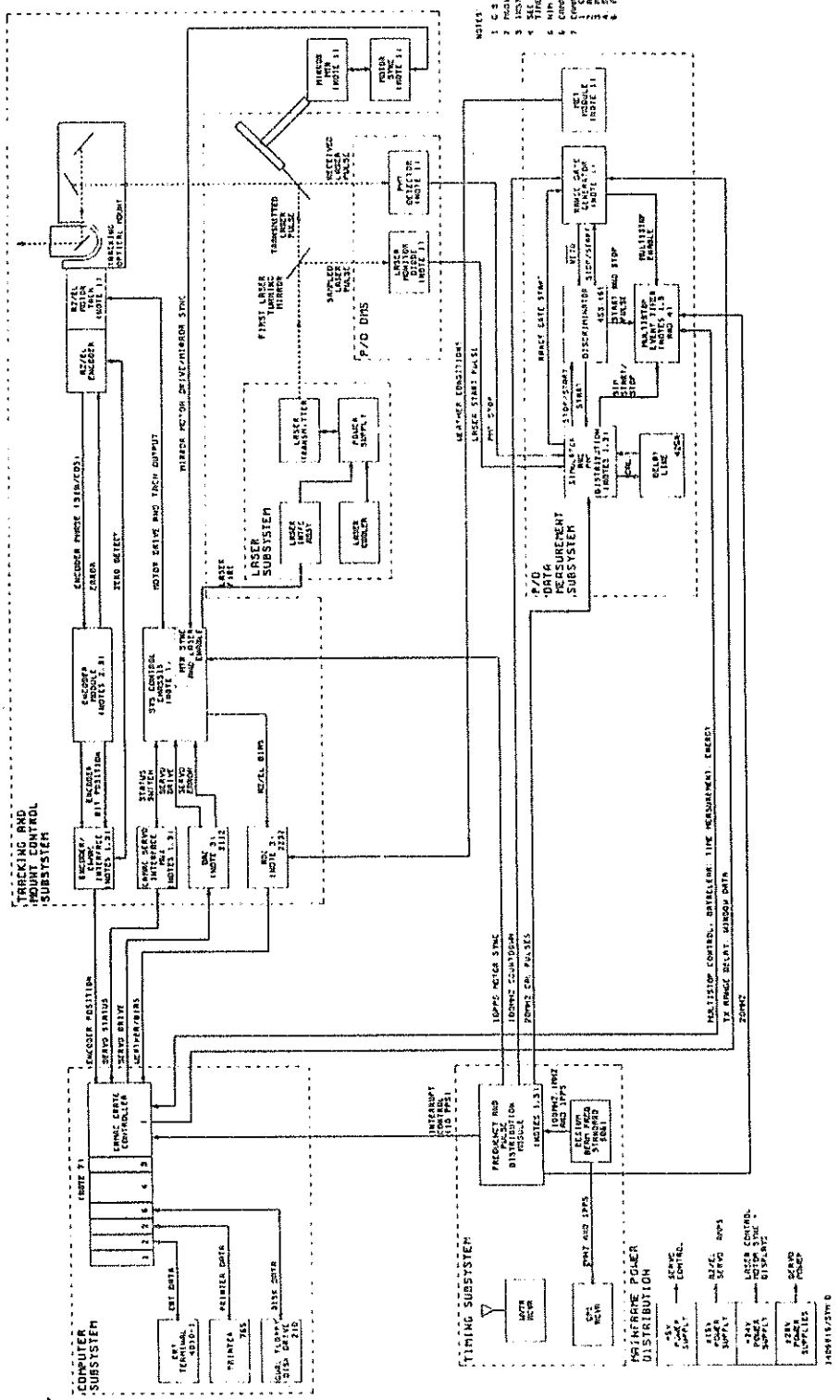

Fig. 9 TLRS-2 Overall Block Diagram

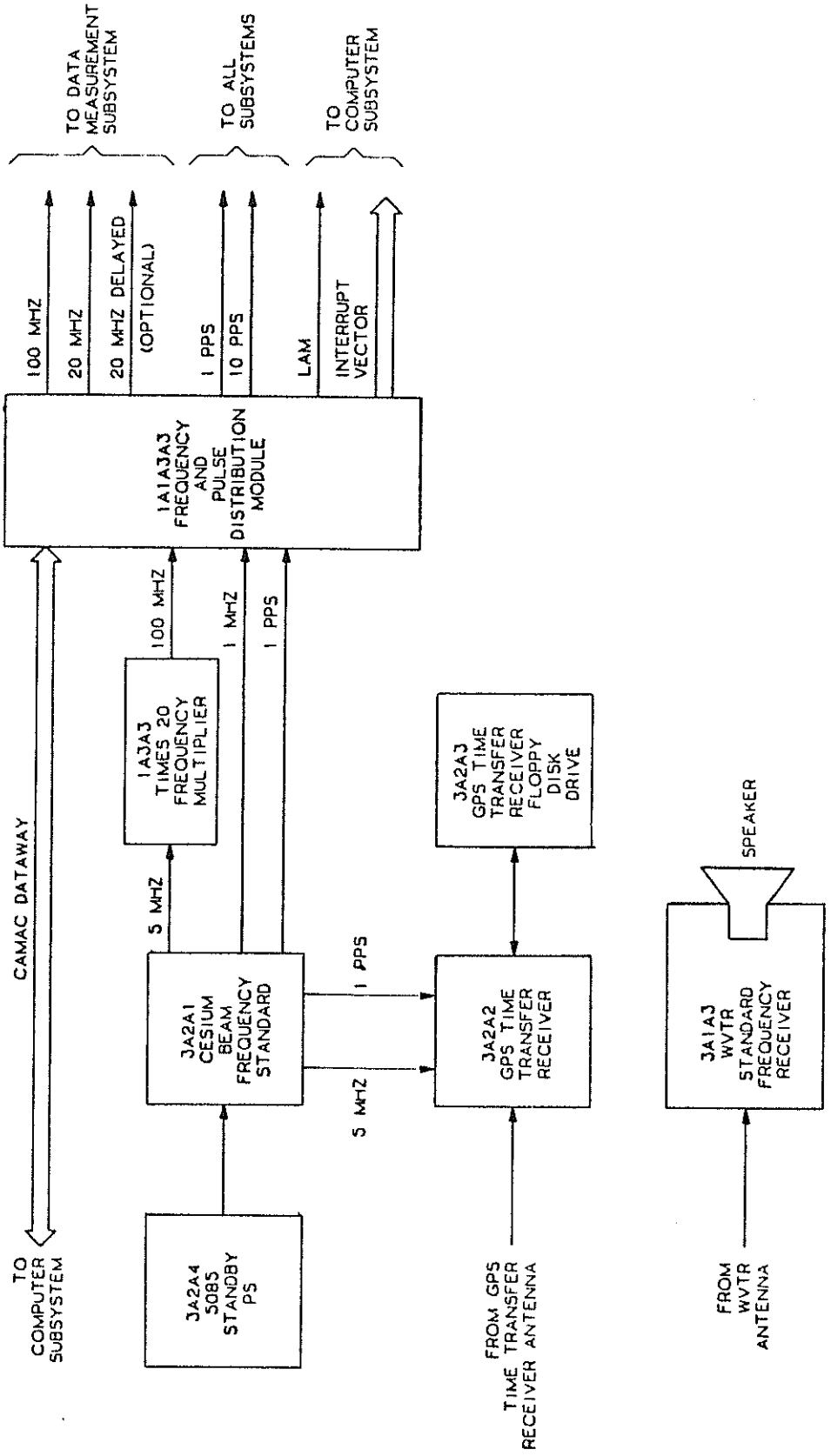

Fig. 10 Timing Subsystem, Simplified Block Diagram

NAVSTAR GPS TIME TRANSFER

EPOCH DAY 57.0 ,1984

SAT ID	TT US	FREQ PP13	AGING PP14/D	RMS NS	PTS USED	PTS FLTRD	FILTER TOL(NS)
1	.000	.00	.0	0	0	0	START 300
3	-15.682	-23.77	.0	74	11	0	PLOT
4	-15.658	-25.50	.0	48	13	0	COMP 300
5	.000	.00	.0	0	0	0	DFIT 1
6	-15.624	-24.09	.0	59	12	0	
8	-15.619	-25.54	.0	60	8	0	
9	.000	.00	.0	0	0	0	
COMP	-15.650	-24.53	.0	68	44	0	

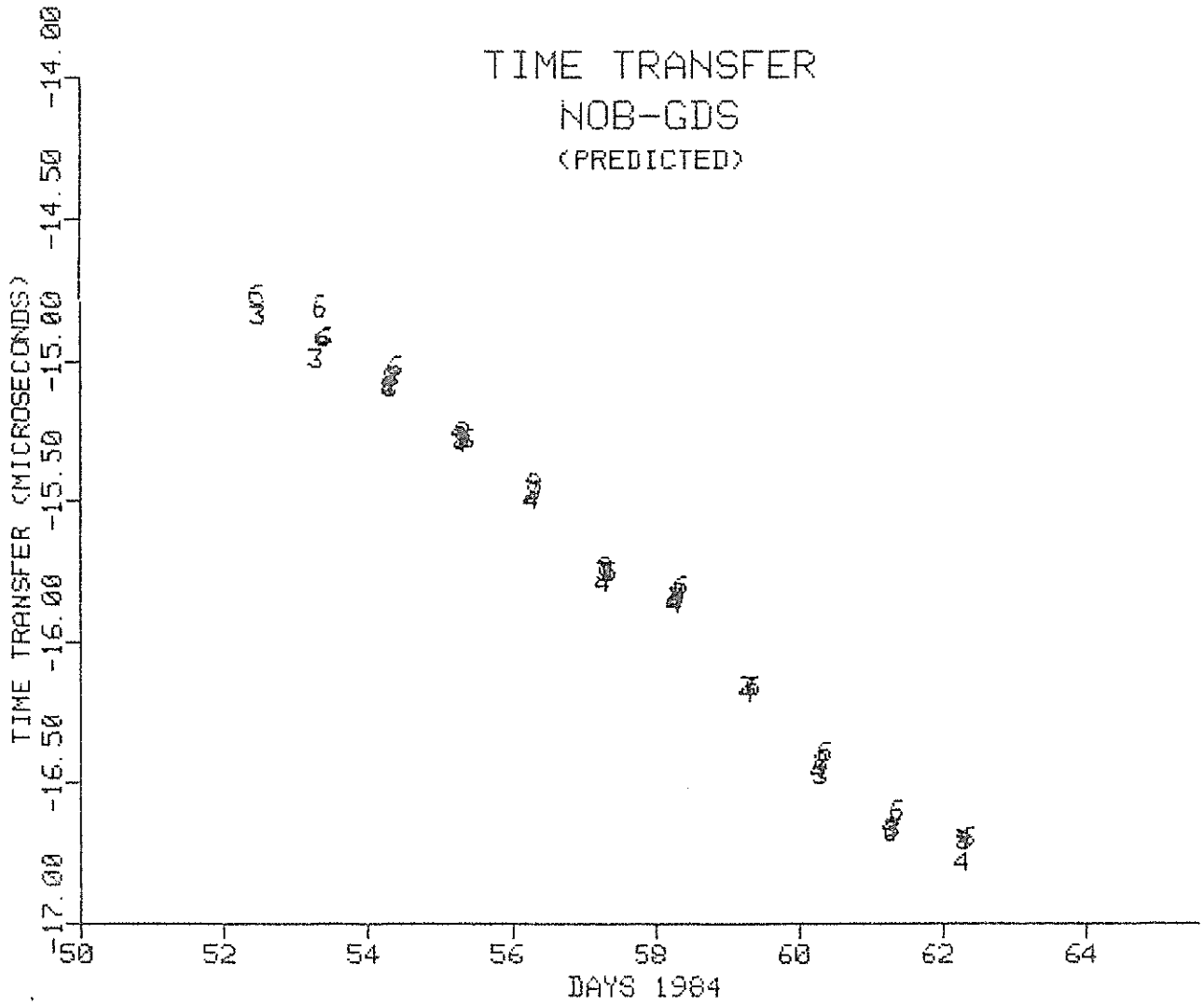

Fig. 11 NAVSTAR GPS Time Transfer

NAVSTAR GPS TIME TRANSFER

EPOCH DAY 57.0 , 1984

SAT ID	TT US	FREQ PP13	AGING PP14/D	RMS NS	PTS USED	PTS FLTRD	FILTER TOL(NS)
1	.000	.00	.0	0	0	0	STAT 300
3	-15.728	-27.63	.0	81	10	0	PLOT
4	-15.631	-23.79	.0	72	10	0	COMP 300
5	.000	.00	.0	0	0	0	DFIT 1
6	-15.625	-29.01	.0	87	10	0	
8	-15.726	-25.05	.0	56	8	0	
9	.000	.00	.0	0	0	0	
COMP	-15.671	-26.09	.0	104	38	0	

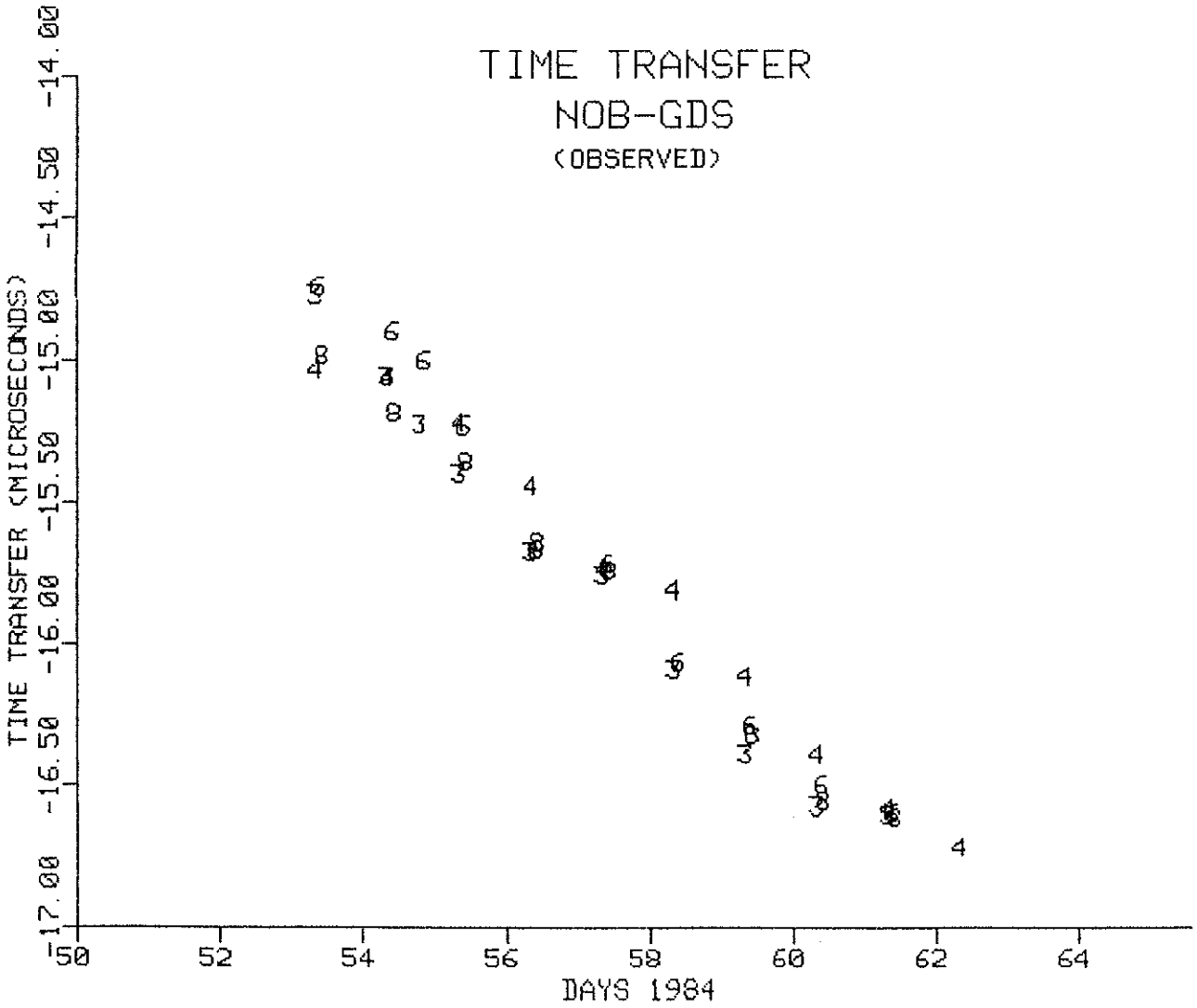

Fig. 12 NAVSTAR GPS Time Transfer

NAVSTAR GPS TIME TRANSFER

EPOCH DAY 99.5 , 1984

SAT ID	TT US	FREQ PP13	AGING PP14/D	RMS NS	PTS USED	PTS FLTRD
1	.000	.00	.0	0	0	0
3	-1.652	45.47	.0	6036	54	0
4	-3.079	42.59	.0	7191	16	0
5	.000	.00	.0	0	0	0
6	-1.205	46.06	.0	6013	52	0
8	-1.192	51.31	.0	6427	38	0
9	.000	.00	.0	0	0	0
COMP	-1.532	47.27	.0	6269	160	0

FILTER TOL(NS)
STAT 3000
PLOT
COMP 3000
DFIT 1

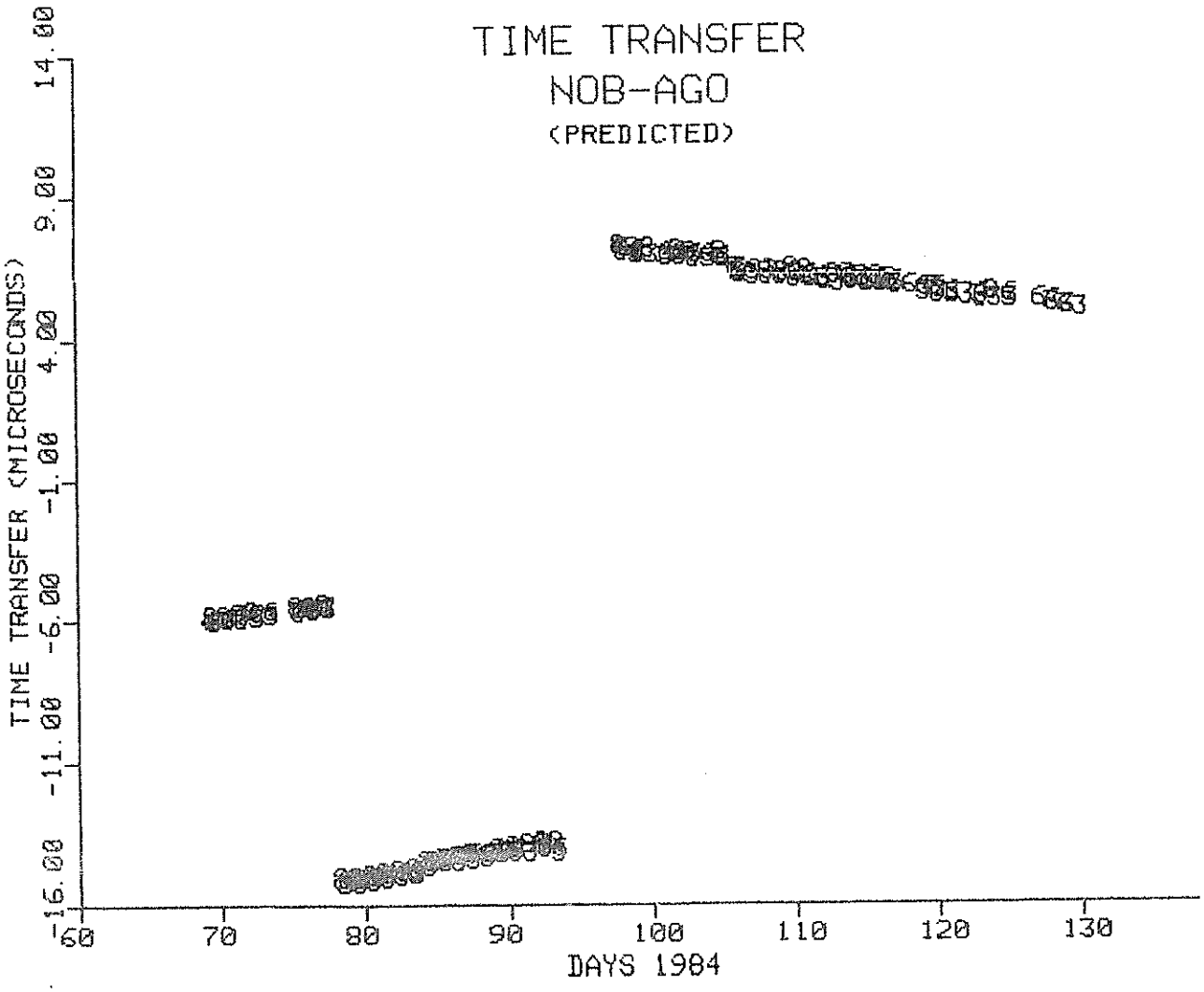

Fig. 13 NAVSTAR GPS Time Transfer

NAVSTAR GPS TIME TRANSFER

EPOCH DAY 99.5 , 1984

SAT ID	TT US	FREQ PP13	AGING PP14/D	RMS NS	PTS USED	PTS FLTRD
1	.000	.00	.0	0	0	0
3	-1.672	45.40	.0	6101	51	0
4	-2.733	56.86	.0	6958	14	0
5	.000	.00	.0	0	0	0
6	-1.580	45.60	.0	5855	49	0
8	-2.037	51.45	.0	6235	34	0
9	.000	.00	.0	0	0	0
COMP	-1.937	47.93	.0	6186	148	0

FILTER TOL(NS)
STAT 3000
PLOT
COMP 3000
DFIT 1

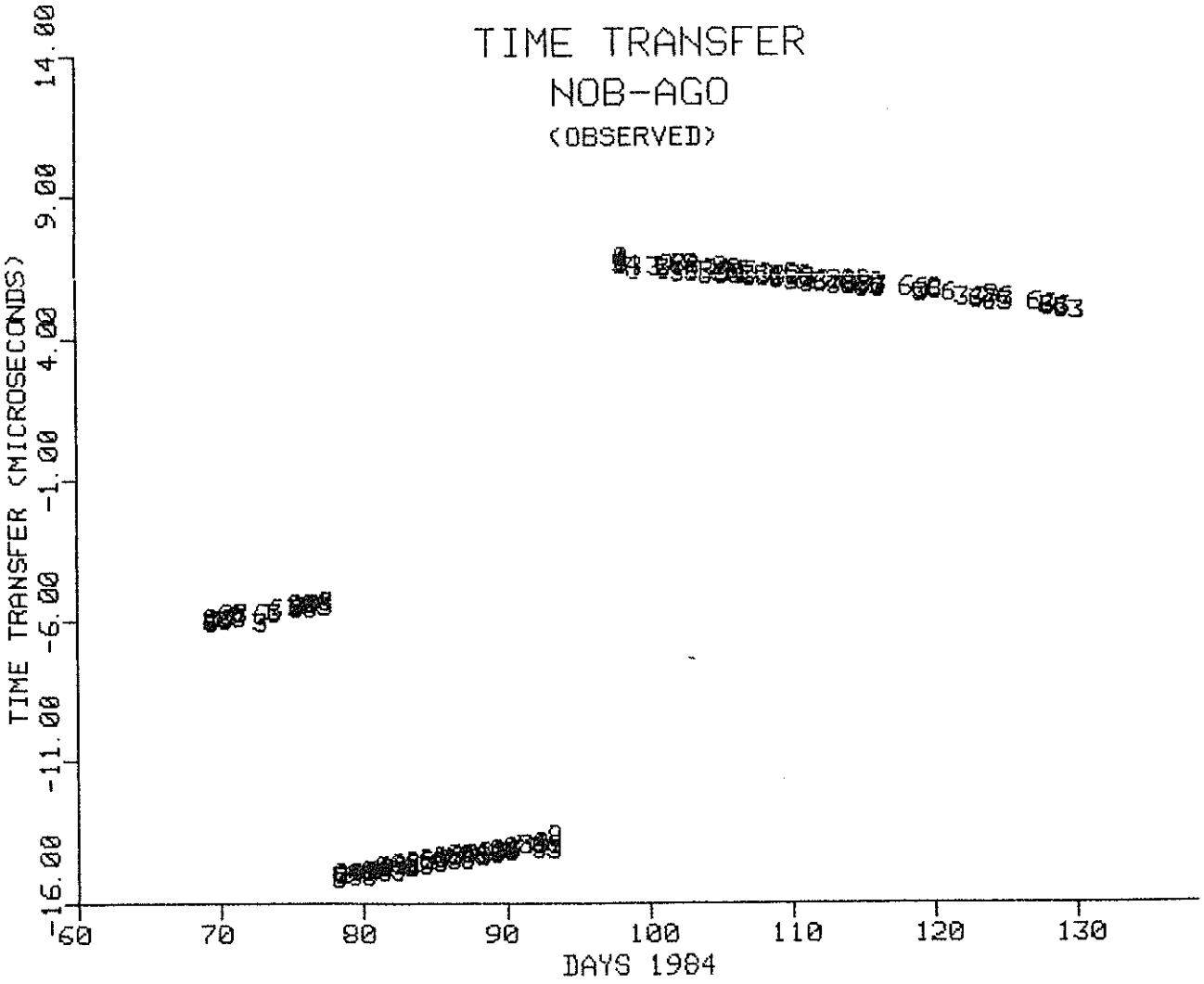

Fig. 14 NAVSTAR GPS Time Transfer

NAVSTAR GPS TIME TRANSFER

EPOCH DAY 73.0 ,1984

SAT ID	TT US	FREQ PP13	AGING PP14/D	RMS NS	PTS USED	PTS FLTRD
1	.000	.00	.0	0	0	0
3	-5.747	7.09	.0	17	8	0
4	.000	.00	.0	0	0	0
5	.000	.00	.0	0	0	0
6	-5.632	7.20	.0	44	8	0
8	-5.534	6.66	.0	14	7	0
9	.000	.00	.0	0	0	0
COMP	-5.633	7.12	.0	88	27	0

FILTER TOL(NS)
STAT 300
PLOT
COMP 300
DFIT 1

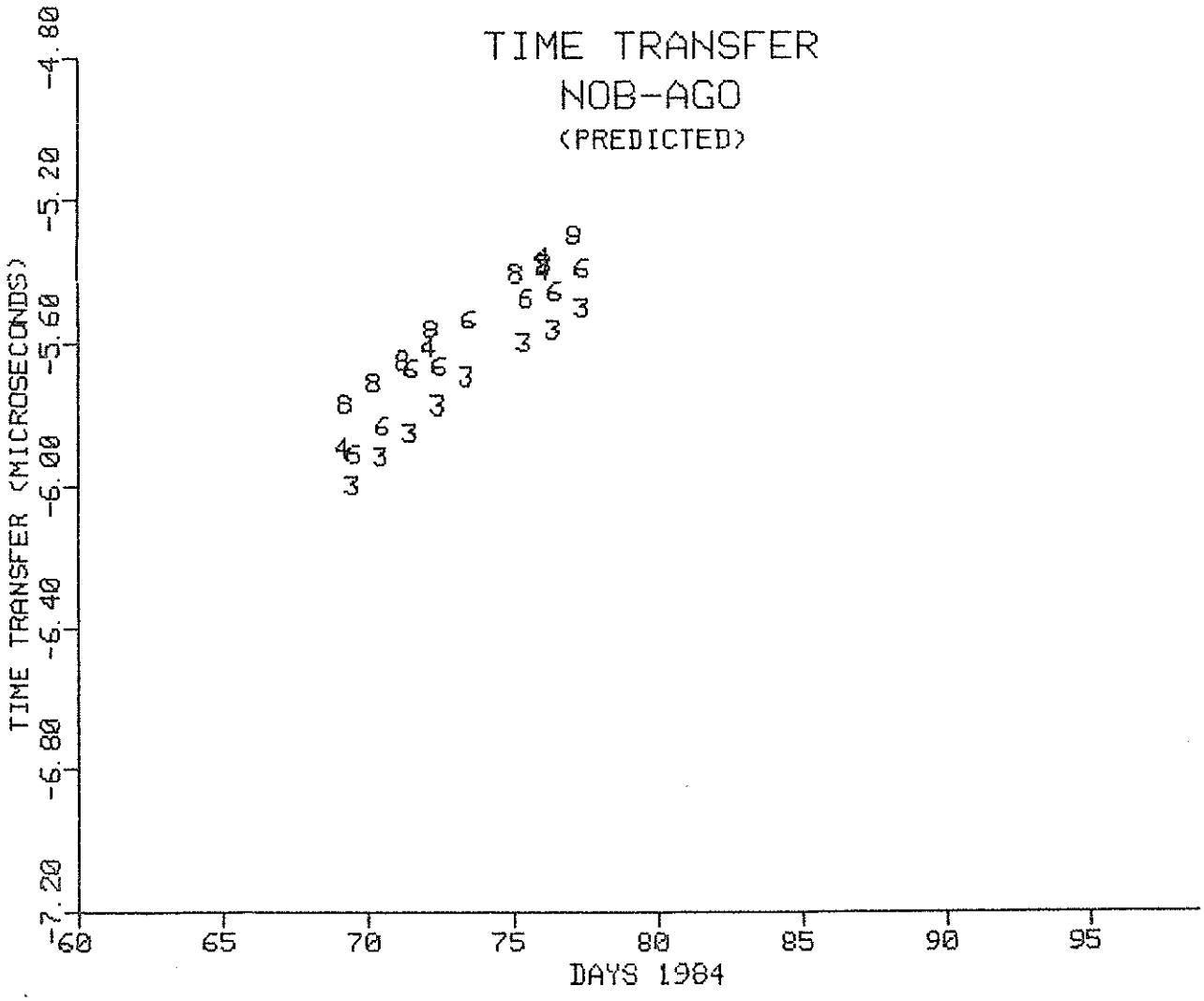

Fig. 15 NAVSTAR GPS Time Transfer

NAVSTAR GPS TIME TRANSFER

EPOCH DAY 73.0 ,1984

SAT ID	TT US	FREQ PP13	AGING PP14/D	RMS NS	PTS USED	PTS FLTRD	FILTER TOL(NS)
1	.000	.00	.0	0	0	0	STAT 300
3	-5.680	8.75	.0	17	7	0	PLOT
4	.000	.00	.0	0	0	0	COMP 300
5	.000	.00	.0	0	0	0	DFIT 1
6	-5.579	9.25	.0	42	8	0	
8	-5.501	8.08	.0	10	6	0	
9	.000	.00	.0	0	0	0	
COMP	-5.590	8.87	.0	74	23	0	

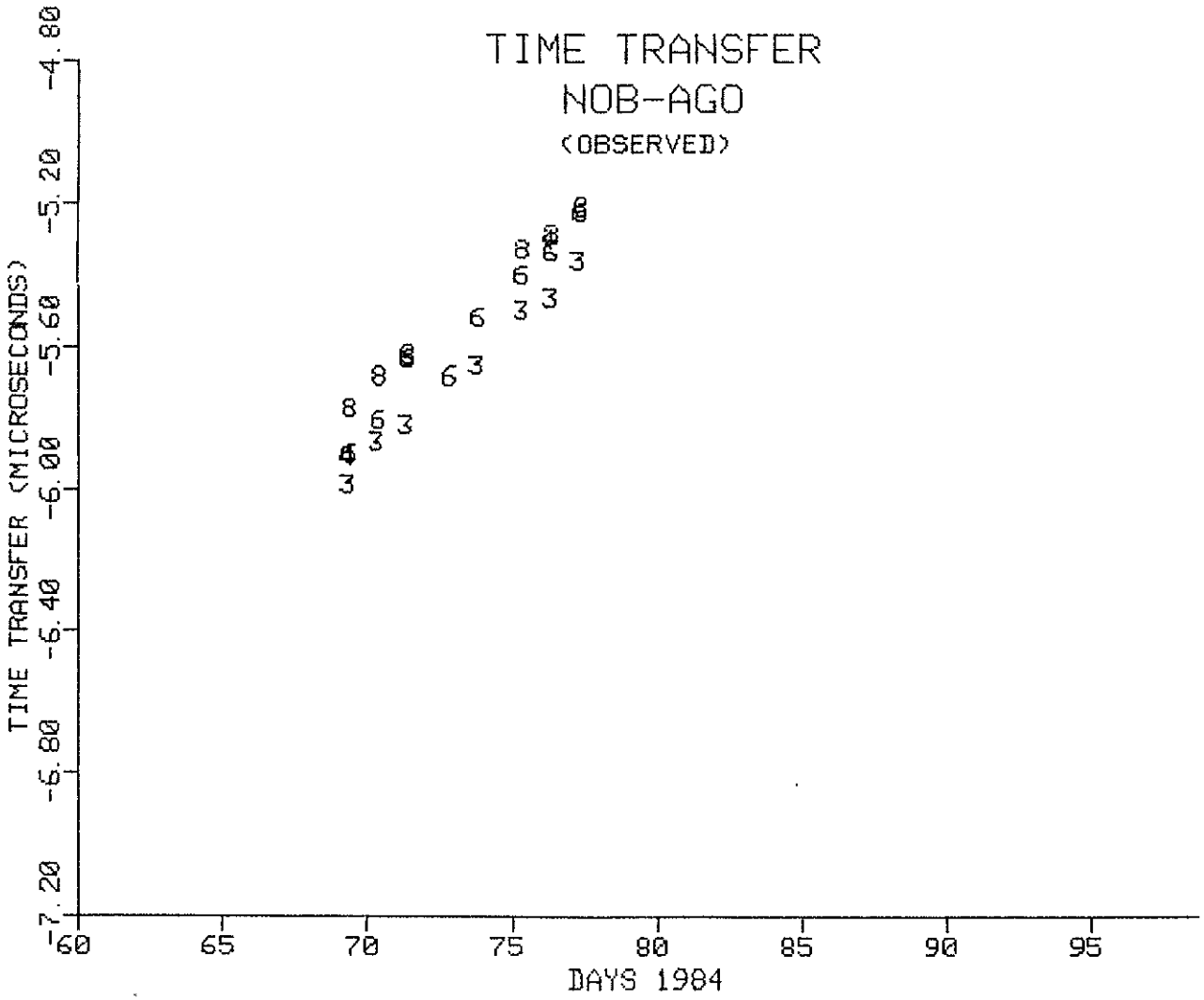

Fig. 16 NAVSTAR GPS Time Transfer

NAVSTAR GPS TIME TRANSFER

EPOCH DAY 85.0 , 1984

SAT ID	TT US	FREQ PP13	AGING PP14/D	RMS NS	PTS USED	PTS FLTRD	FILTER TOL(NS)
1	.000	.00	.0	0	0	0	STAT 300
3	-14.608	11.36	.0	69	15	0	PLOT
4	-14.412	11.37	.0	46	9	0	COMP 300
5	.000	.00	.0	0	0	0	DFIT 1
6	-14.465	11.44	.0	79	14	0	
8	-14.393	11.34	.0	60	14	0	
9	.000	.00	.0	0	0	0	
COMP	-14.475	11.33	.0	112	52	0	

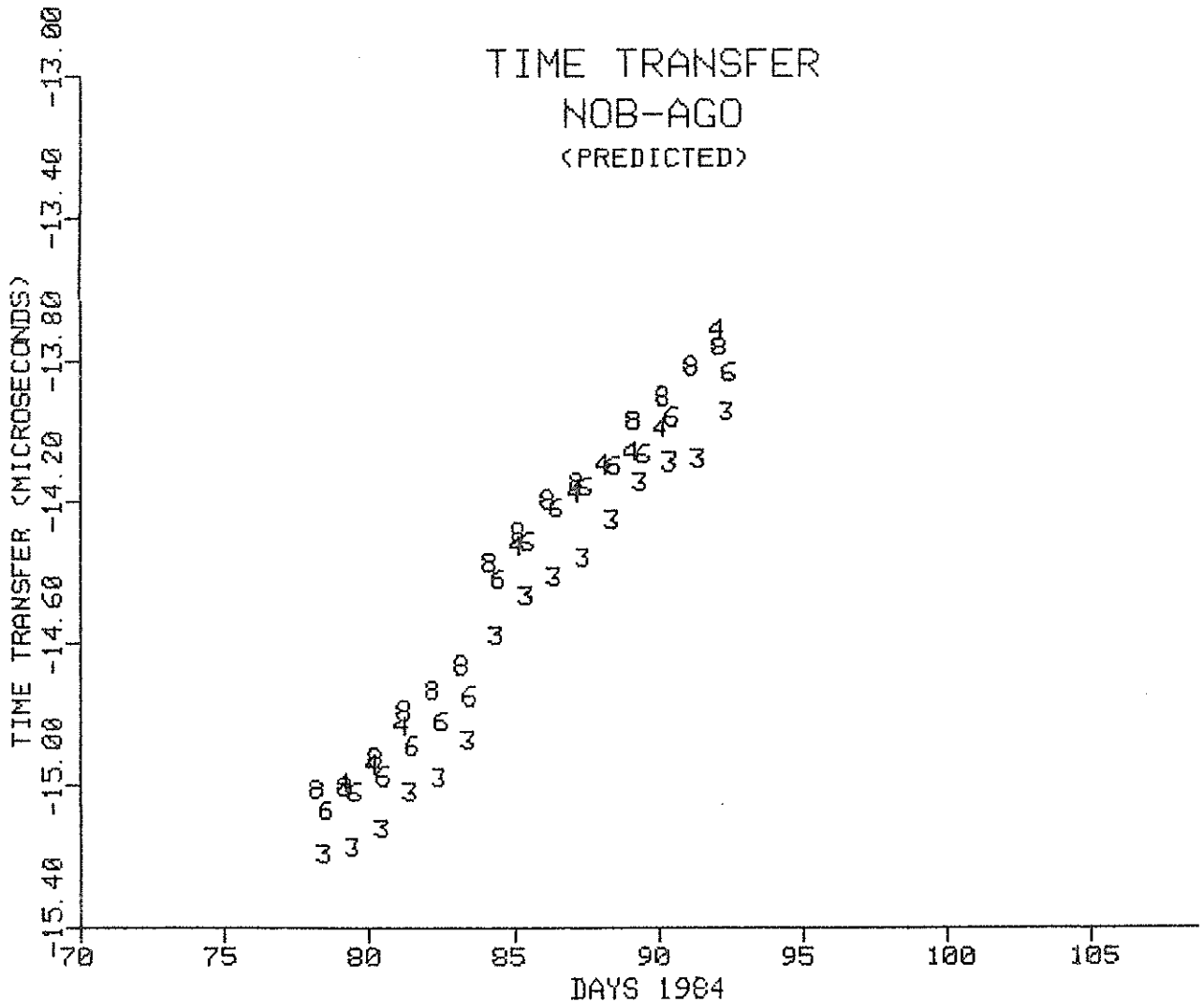

Fig. 17 NAVSTAR GPS Time Transfer

NAVSTAR GPS TIME TRANSFER

EPOCH DAY 85.0 , 1984

SAT ID	TT US	FREQ PP13	AGING PP14/D	RMS NS	PTS USED	PTS FLTRD	FILTER TOL(NS)
1	.000	.00	.0	0	0	0	STAT 300
3	-14.556	9.85	.0	58	15	0	PLOT
4	-14.426	9.24	.0	40	9	0	COMP 300
5	.000	.00	.0	0	0	0	DFIT 1
6	-14.423	9.04	.0	32	14	0	
8	-14.374	9.17	.0	24	14	0	
9	.000	.00	.0	0	0	0	
COMP	-14.448	9.33	.0	83	52	0	

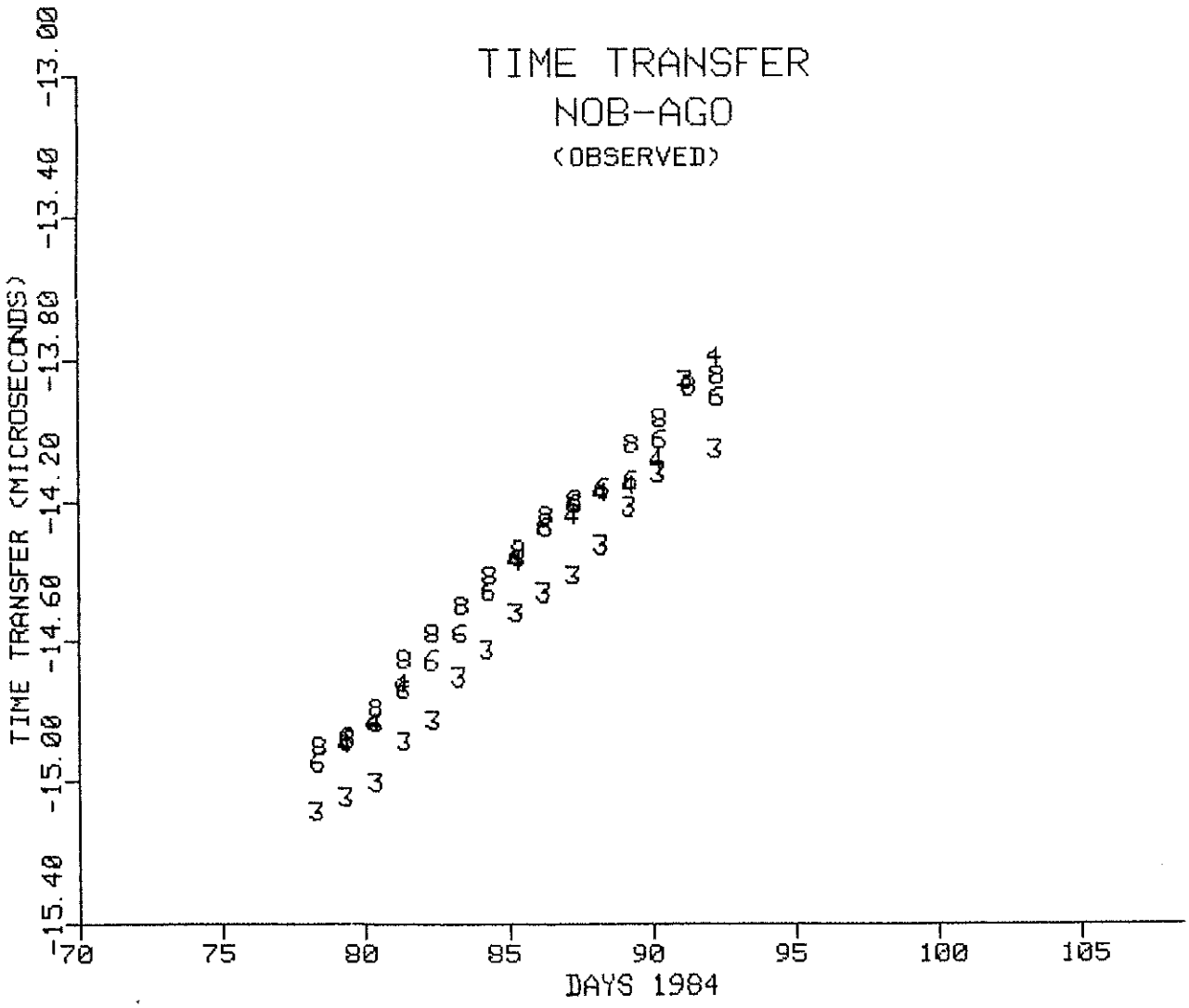

Fig. 18 NAVSTAR GPS Time Transfer

NAVSTAR GPS TIME TRANSFER

EPOCH DAY 114.0, 1984

SAT ID	TT US	FREQ PP13	AGING PP14/D	RMS NS	PTS USED	PTS FLTRD	FILTER TOL(NS)
1	.000	.00	.0	0	0	0	STAT 300
3	6.092	-7.35	.0	96	30	0	PLOT
4	.000	.00	.0	0	0	0	COMP 300
5	.000	.00	.0	0	0	0	DFIT 1
6	6.202	-7.48	.0	114	29	0	
8	6.281	-7.82	.0	101	16	0	
9	.000	.00	.0	0	0	0	
COMP	6.174	-7.62	.0	129	78	0	

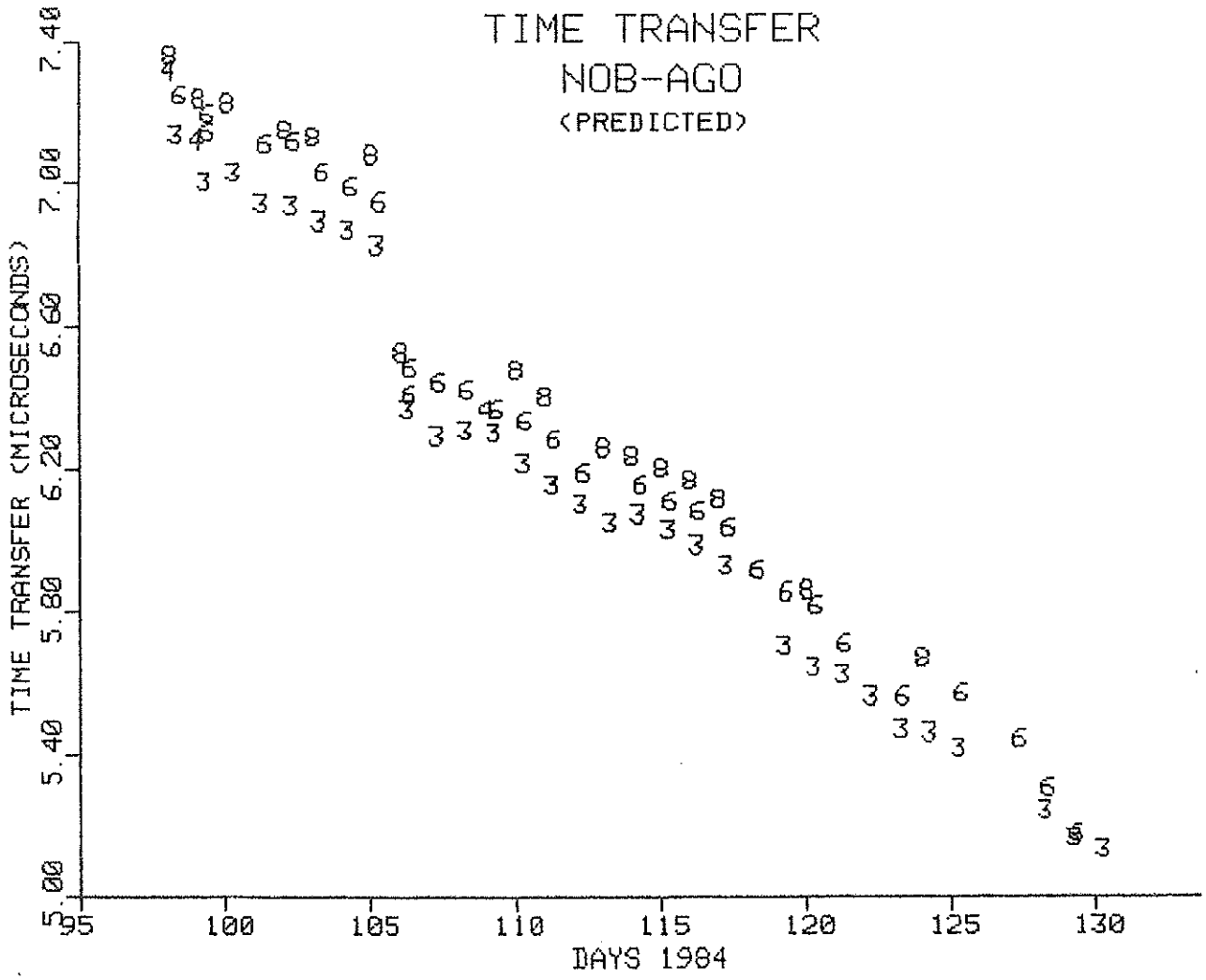

Fig. 19 NAVSTAR GPS Time Transfer

NAVSTAR GPS TIME TRANSFER

EPOCH DAY 114.0, 1984

SAT ID	TT US	FREQ PP13	AGING PP14/D	RMS NS	PTS USED	PTS FLTRD	FILTER TOL(NS)
1	.000	.00	.0	0	0	0	STAT 300
3	5.909	-5.81	.0	40	27	0	PLOT
4	.000	.00	.0	0	0	0	COMP 300
5	.000	.00	.0	0	0	0	DFIT 1
6	6.034	-5.85	.0	38	26	0	
8	6.130	-5.81	.0	26	13	0	
9	.000	.00	.0	0	0	0	
COMP	6.001	-5.87	.0	91	69	0	

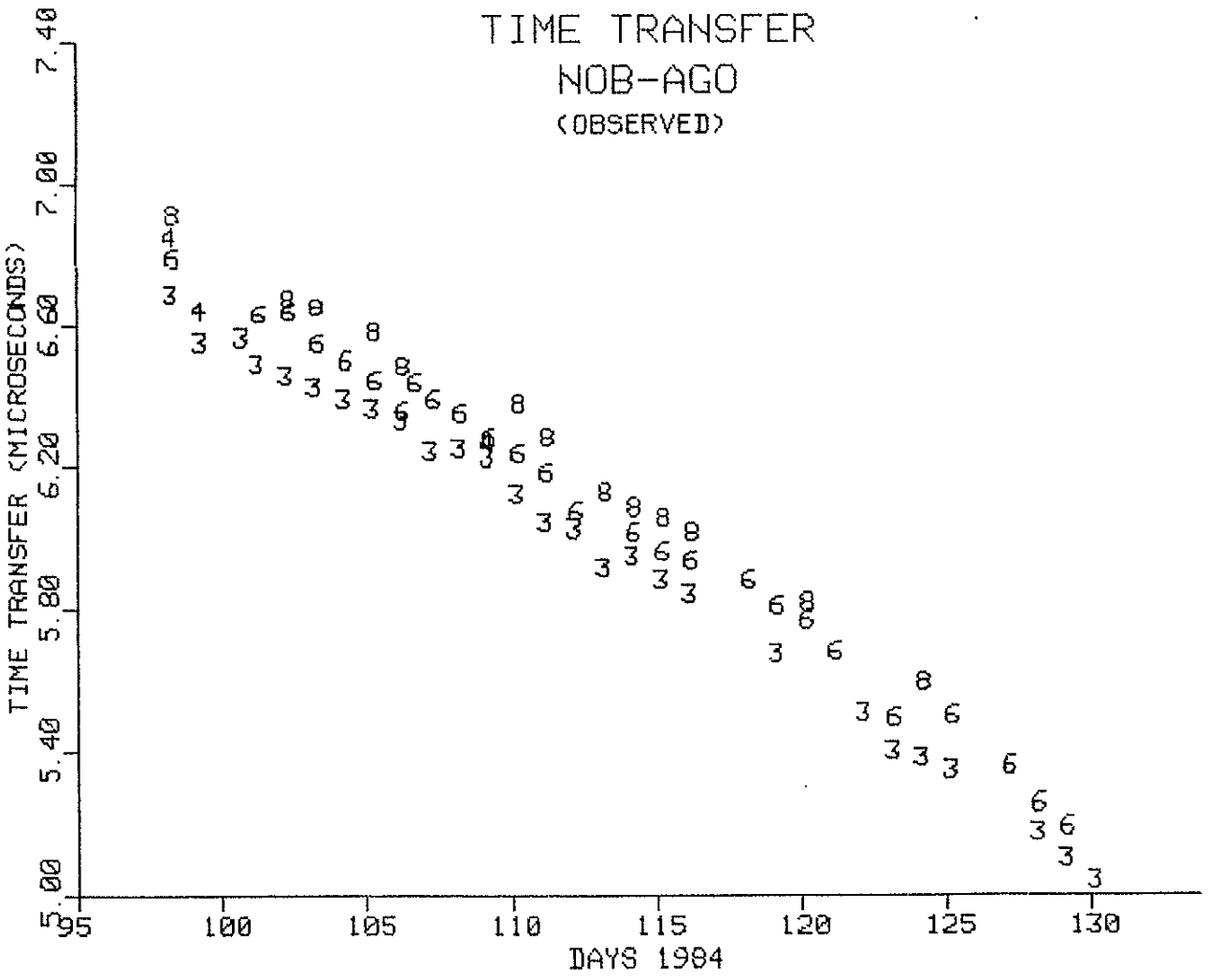

Fig. 20 NAVSTAR GPS Time Transfer

NAVSTAR GPS TIME TRANSFER

EPOCH DAY 155.0, 1984

SAT ID	TT US	FREQ PP13	AGING PP14/D	RMS NS	PTS USED	PTS FLTRD	FILTER TOL(NS)
1	.000	.00	.0	0	0	0	STAT 300
3	2.336	-11.14	.0	183	34	0	PLOT
4	.000	.00	.0	0	0	0	COMP 300
5	.000	.00	.0	0	0	0	DFIT 1
6	2.499	-13.90	.0	161	34	0	
8	2.524	-14.27	.0	186	27	0	
9	.000	.00	.0	0	0	0	
COMP	2.449	-13.05	.0	232	95	0	

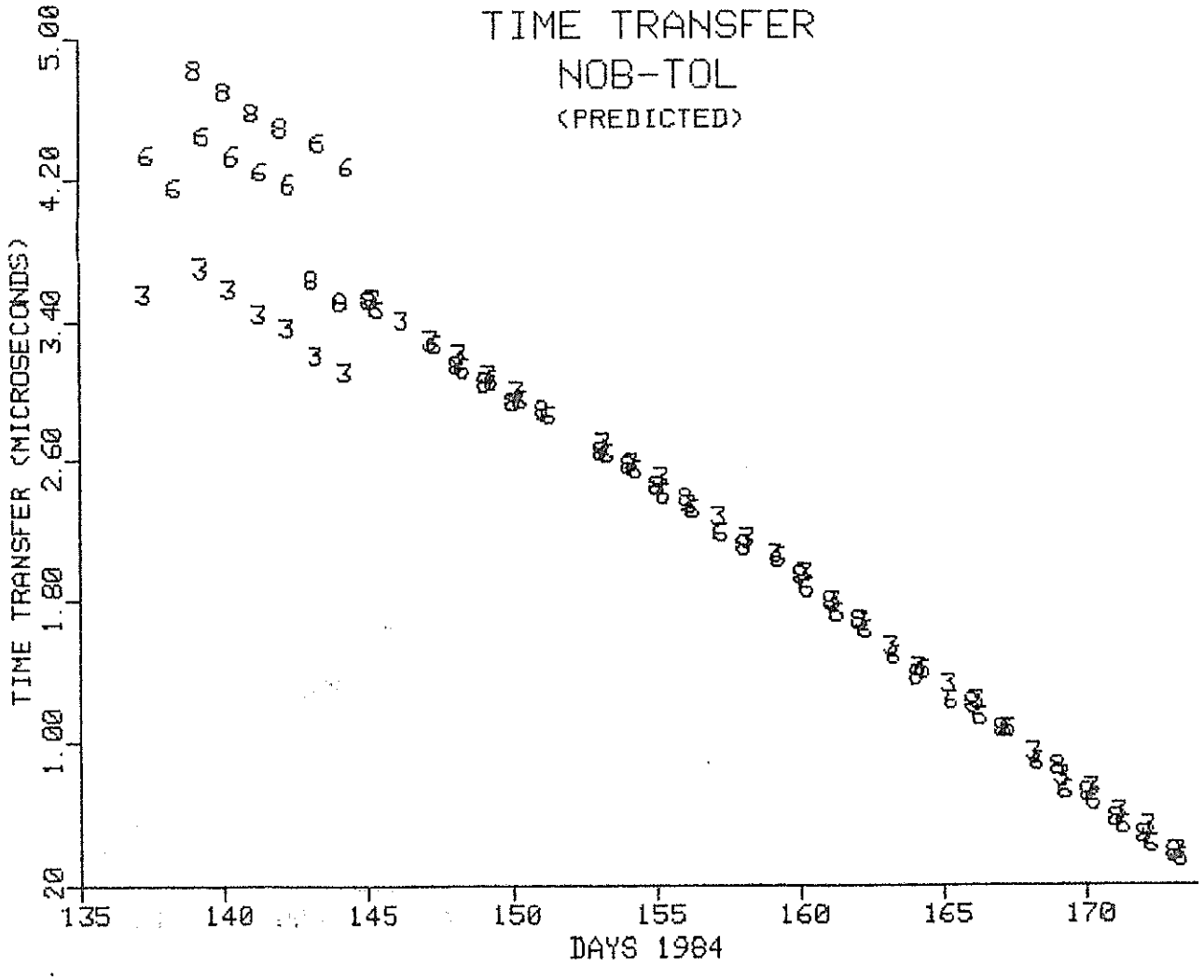

Fig. 21 NAVSTAR GPS Time Transfer

NAVSTAR GPS TIME TRANSFER

EPOCH DAY 155.0, 1984

SAT ID	TT US	FREQ PP13	AGING PP14/D	RMS NS	PTS USED	PTS FLTRD
1	.000	.00	.0	0	0	0
3	2.312	-11.06	.0	156	34	0
4	.000	.00	.0	0	0	0
5	.000	.00	.0	0	0	0
6	2.486	-14.03	.0	139	34	0
8	2.490	-13.94	.0	185	24	0
9	.000	.00	.0	0	0	0
COMP	2.426	-12.92	.0	219	92	0

FILTER TOL(NS)
STAT 300
PLOT
COMP 300
DFIT 1

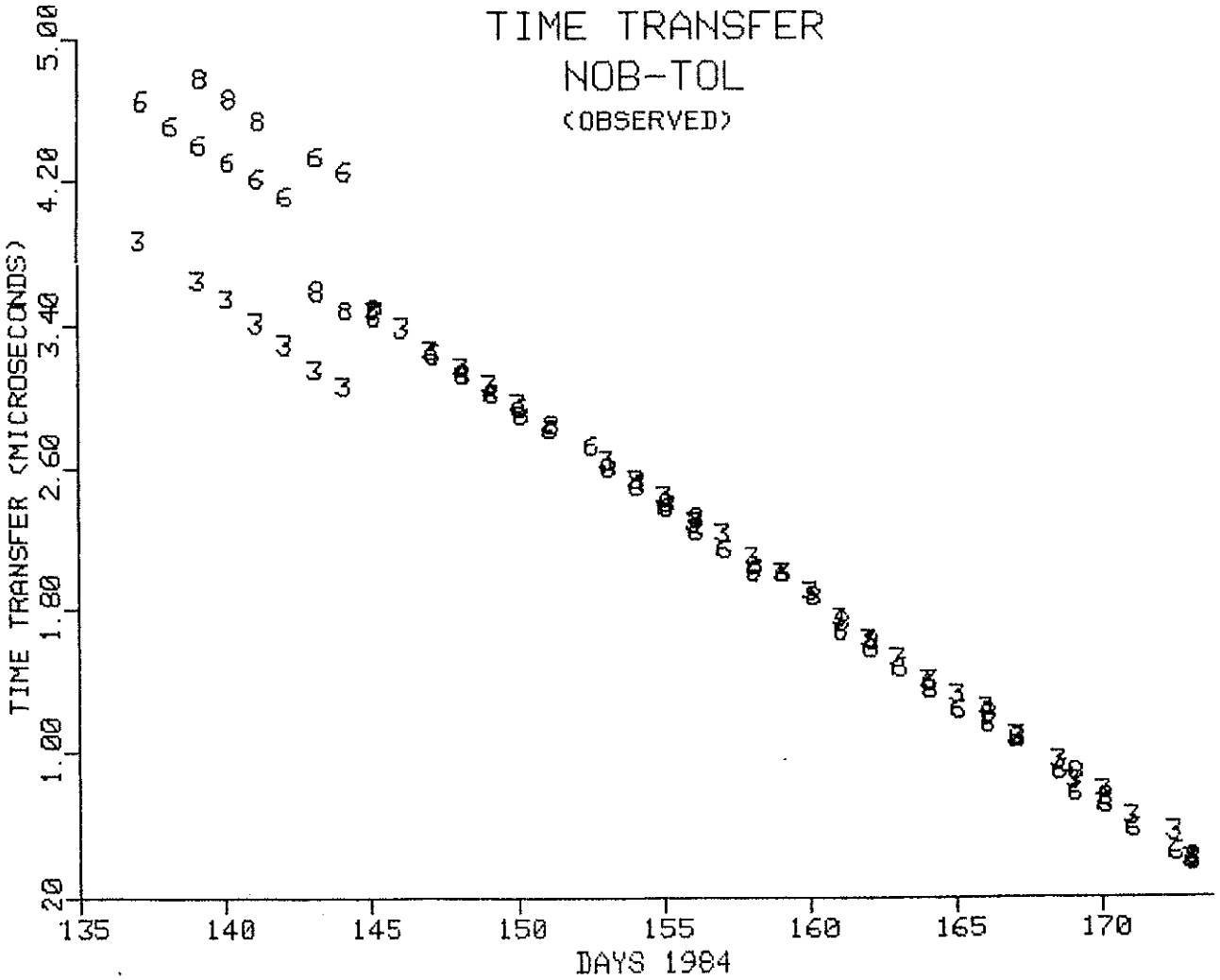

Fig. 22 NAVSTAR GPS Time Transfer

NAVSTAR GPS TIME TRANSFER

EPOCH DAY 159.0, 1984

SAT ID	TT US	FREQ PP13	AGING PP14/D	RMS NS	PTS USED	PTS FLTRD
1	.000	.00	.0	0	0	0
3	2.024	-13.08	.0	37	27	0
4	.000	.00	.0	0	0	0
5	.000	.00	.0	0	0	0
6	1.981	-13.21	.0	38	26	0
8	1.990	-13.07	.0	40	21	0
9	.000	.00	.0	0	0	0
COMP	1.999	-13.12	.0	43	74	0

FILTER TOL(NS)
STAT 300
PLOT
COMP 300
DFIT 1

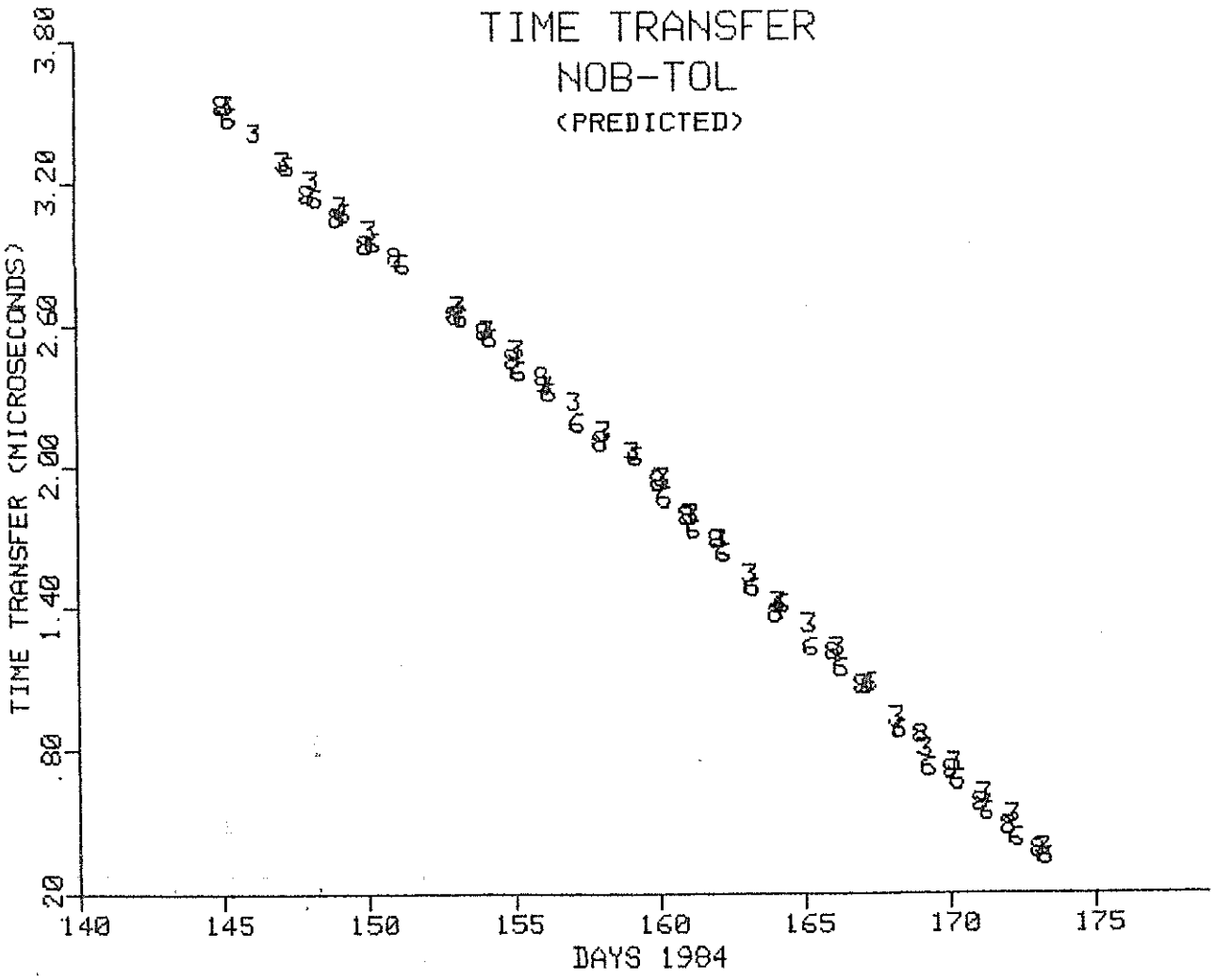

Fig. 23 NAVSTAR GPS Time Transfer

NAVSTAR GPS TIME TRANSFER

EPOCH DAY 159.0, 1984

SAT ID	TT US	FREQ PP13	AGING PP14/D	RMS NS	PTS USED	PTS FLTRD	FILTER TOL(NS)
1	.000	.00	.0	0	0	0	STAT 300
3	1.994	-12.71	.0	25	27	0	PLOT
4	.000	.00	.0	0	0	0	COMP 300
5	.000	.00	.0	0	0	0	DFIT 1
6	1.951	-12.88	.0	29	26	0	
8	1.981	-12.69	.0	25	19	0	
9	.000	.00	.0	0	0	0	
COMP	1.975	-12.77	.0	33	72	0	

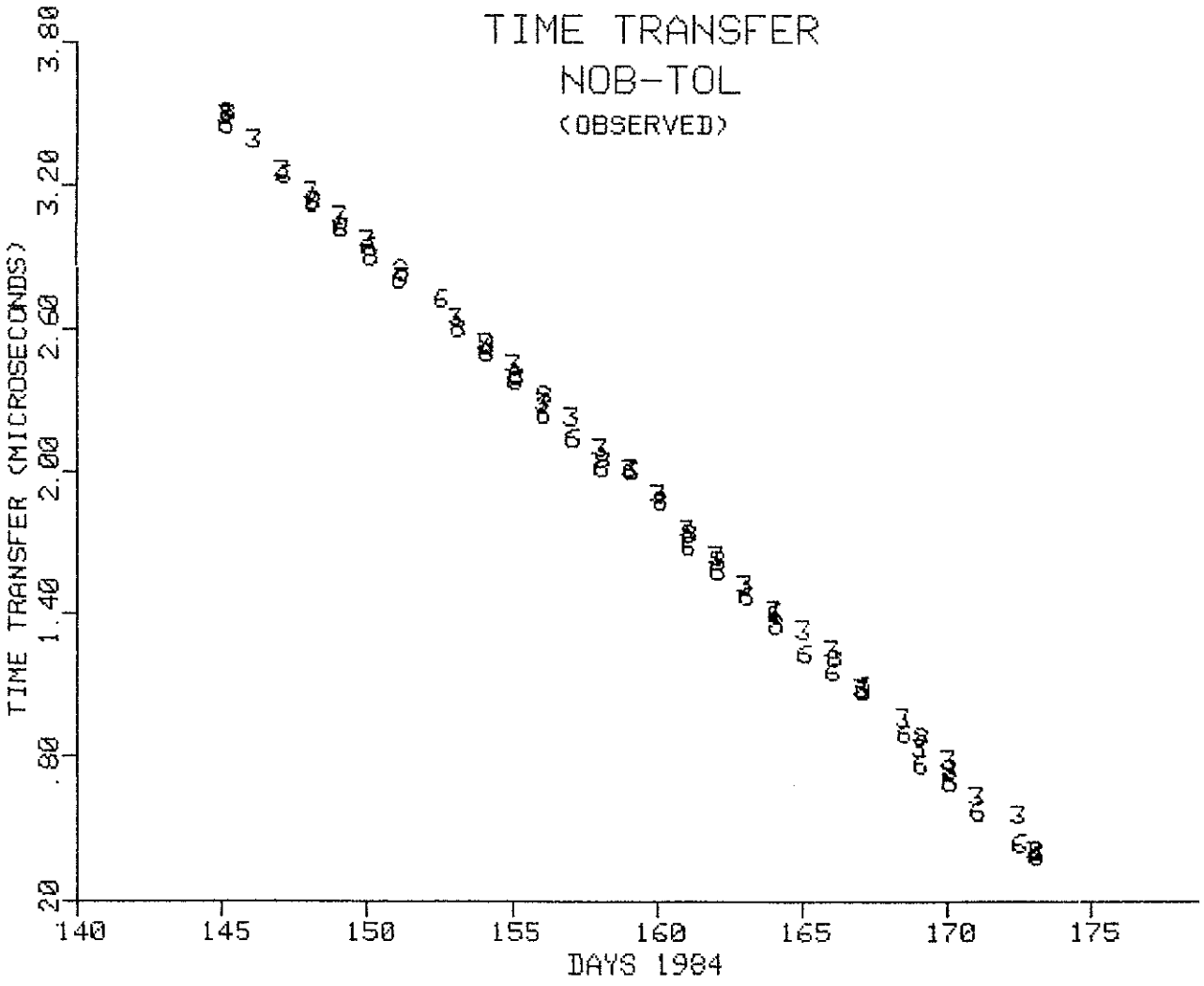

Fig. 24 NAVSTAR GPS Time Transfer

NAVSTAR GPS TIME TRANSFER

EPOCH DAY 312.0, 1983

SAT ID	TT US	FREQ PP13	AGING PP14/D	RMS NS	PTS USED	PTS FLTRD	FILTER TOL(NS)
1	.000	.00	.0	0	0	0	STAT 300
3	1.221	.20	.0	858	49	0	PLOT
4	1.078	-.46	.0	595	28	3	COMP 300
5	1.312	-.67	.0	756	14	0	DFIT 1
6	1.306	.53	.0	907	70	0	
8	1.387	1.75	.0	745	21	0	
9	.000	.00	.0	0	0	0	
COMP	1.225	.36	.0	840	183	2	

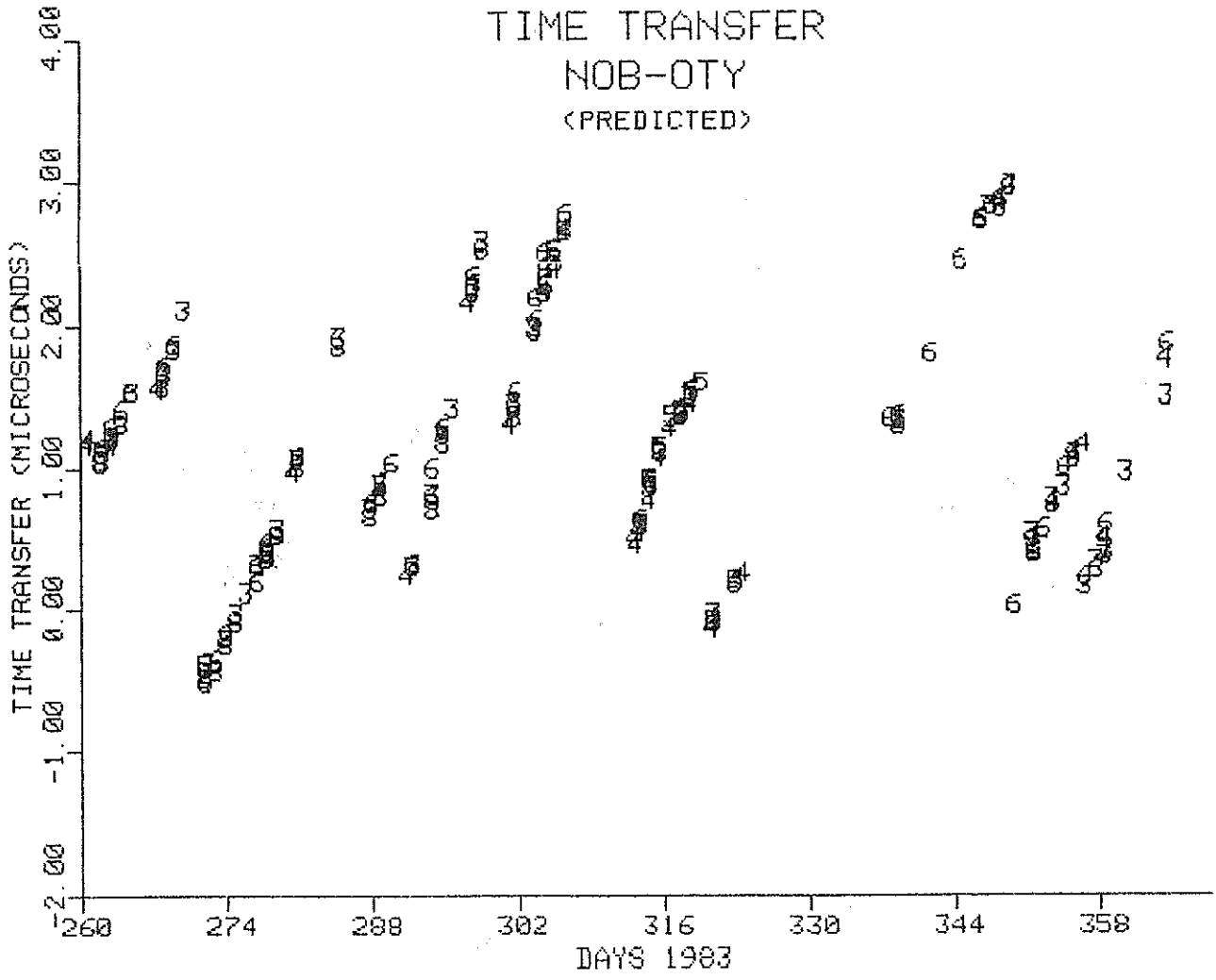

Fig. 25 NAVSTAR GPS Time Transfer

NAVSTAR GPS TIME TRANSFER

EPOCH DAY 312.0, 1983

SAT ID	TT US	FREQ PP13	AGING PP14/D	RMS NS	PTS USED	PTS FLTRD	FILTER TOL(NS)
1	.000	.00	.0	0	0	0	STAT 300
3	1.023	-.58	.0	592	36	8	PLOT
4	1.096	-.73	.0	560	21	4	COMP 300
5	1.280	-.97	.0	707	13	0	DFIT 1
6	1.273	.37	.0	901	65	0	
8	1.234	1.32	.0	796	19	0	
9	.000	.00	.0	0	0	0	
COMP	1.117	-.75	.0	592	136	30	

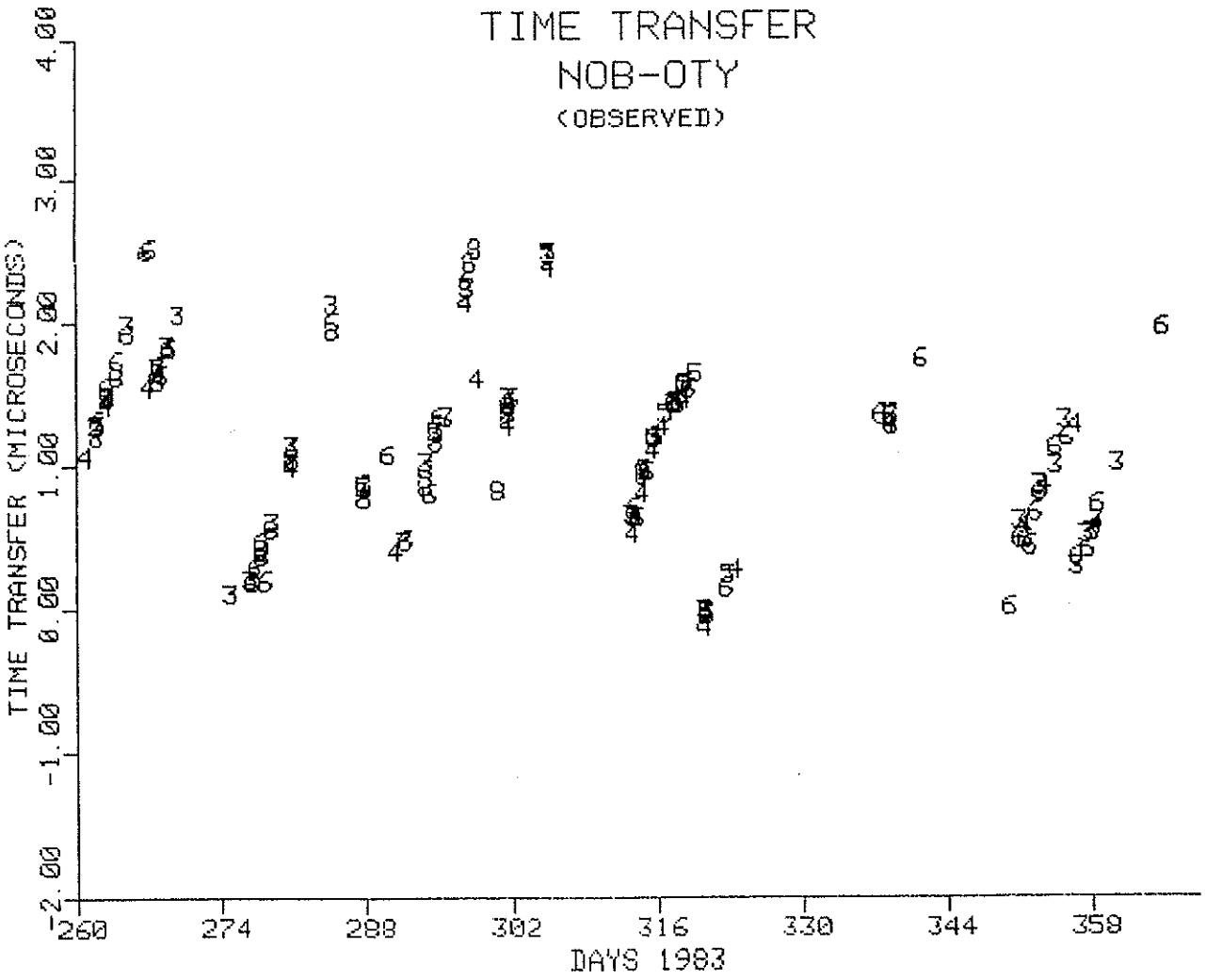

Fig. 26 NAVSTAR GPS Time Transfer

NAVSTAR GPS TIME TRANSFER

EPOCH DAY 277.5, 1983

SAT ID	TT. US.	FREQ PP13	AGING PP14/D	RMS NS	PTS USED	PTS FLTRD	FILTER TOL(NS)
1	.000	.00	.0	0	0	0	STAT 300
3	.478	20.93	.0	95	9	0	PLOT
4	.000	.00	.0	0	0	0	COMP 300
5	.000	.00	.0	0	0	0	DFIT 1
6	.488	20.74	.0	92	10	0	
8	.432	21.01	.0	87	8	0	
9	.000	.00	.0	0	0	0	
COMP	.468	20.87	.0	93	28	0	

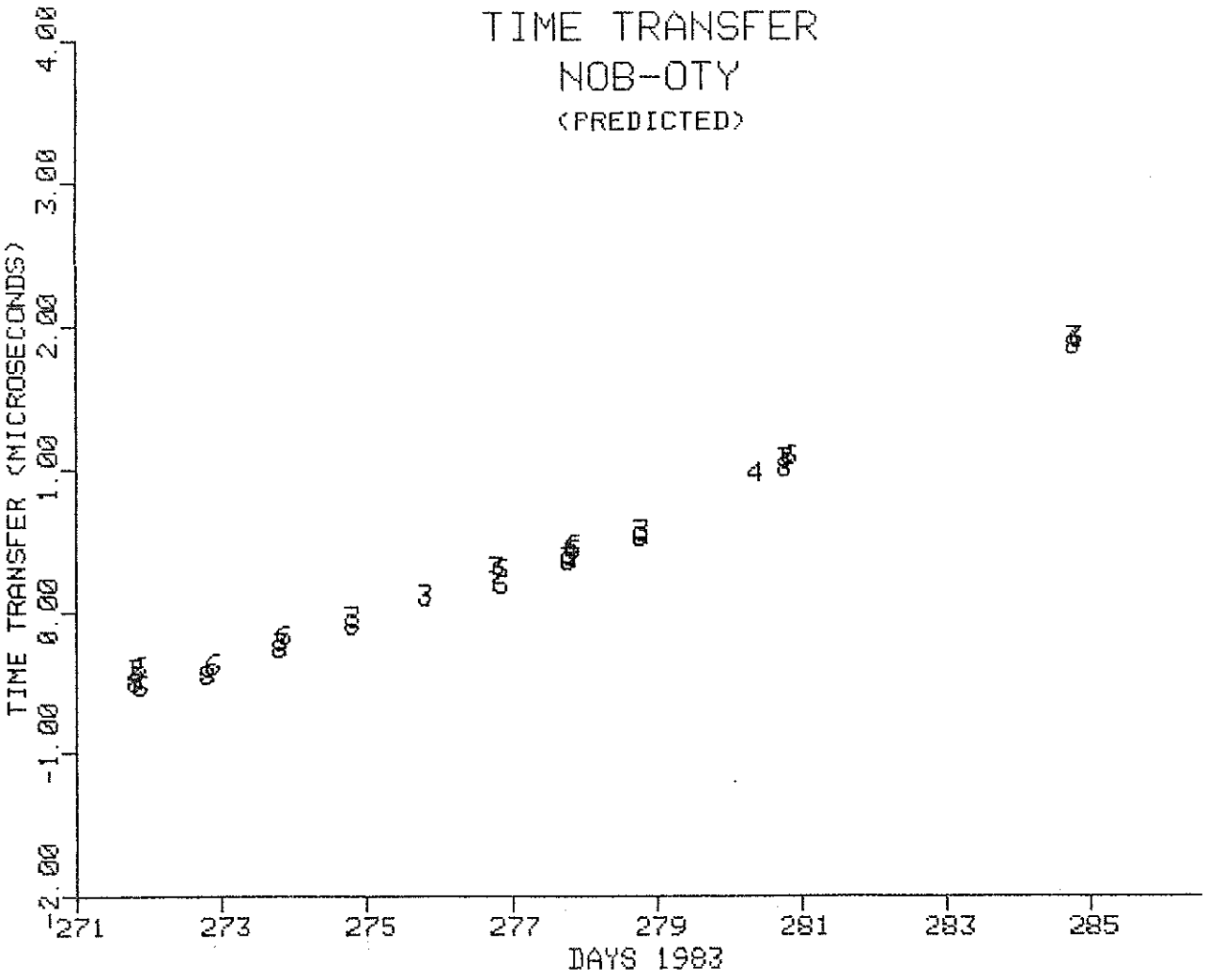

Fig. 27 NAVSTAR GPS Time Transfer

NAVSTAR GPS TIME TRANSFER

EPOCH DAY 277.5, 1983

SAT ID	TT US	FREQ PP13	AGING PP14/D	RMS NS	PTS USED	PTS FLTRD	FILTER TOL(NS)
1	.000	.00	.0	0	0	0	STAT 300
3	.506	23.72	.0	116	7	0	PLOT
4	.000	.00	.0	0	0	0	COMP 300
5	.000	.00	.0	0	0	0	DFIT 1
6	.497	22.71	.0	82	7	0	
8	.427	22.88	.0	65	8	0	
9	.000	.00	.0	0	0	0	
COMP	.476	23.13	.0	98	22	0	

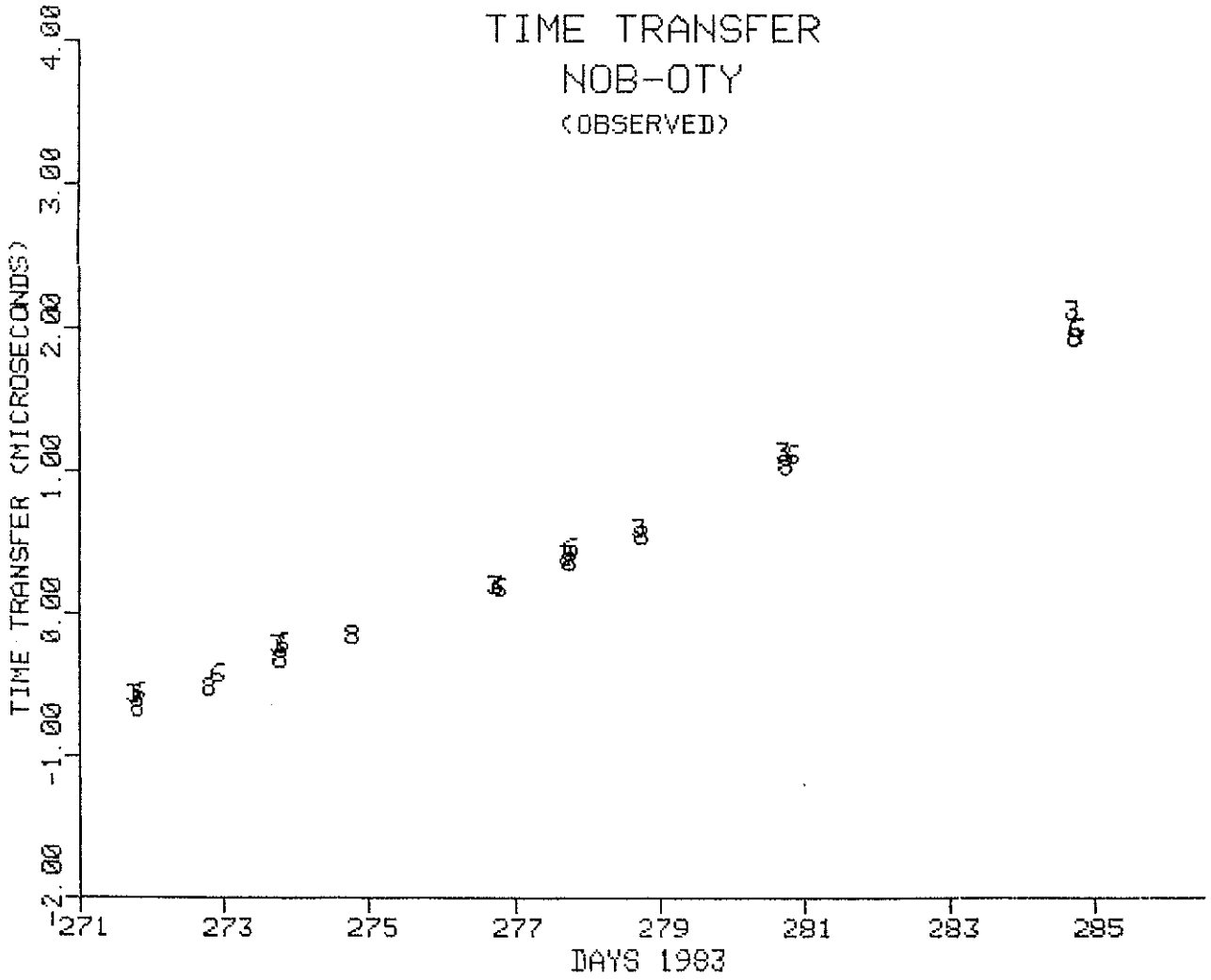

Fig. 28 NAVSTAR GPS Time Transfer

NAVSTAR GPS TIME TRANSFER

EPOCH DAY 57.0 , 1984

SAT ID	TT US	FREQ PP13	AGING PP14/D	RMS NS	PTS USED	PTS FLTRD	FILTER TOL(NS)
1	.000	.00	.0	0	0	0	STAT 300
3	.406	-10.80	.0	58	5	0	PLOT
4	.450	-9.90	.0	74	14	0	COMP 300
5	.000	.00	.0	0	0	0	DFIT 1
6	.451	-10.64	.0	74	5	0	
8	.000	.00	.0	0	0	0	
9	.000	.00	.0	0	0	0	
COMP	.442	-10.22	.0	75	24	0	

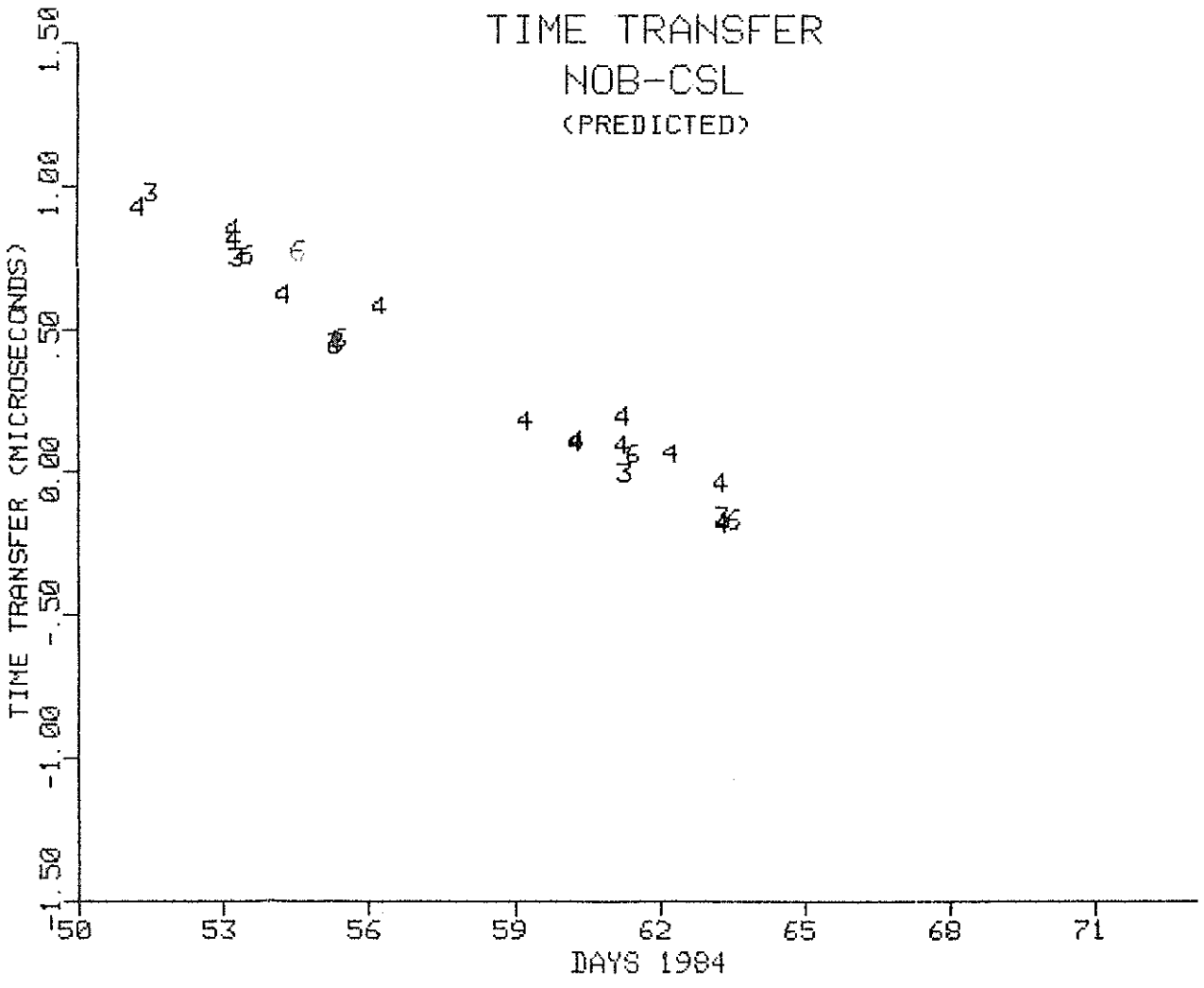

Fig. 29 NAVSTAR GPS Time Transfer

NAVSTAR GPS TIME TRANSFER

EPOCH DAY 57.0 , 1984

SAT ID	TT US	FREQ PP13	AGING PP14/D	RMS NS	PTS USED	PTS FLTRD	FILTER TOL(NS)
1	.000	.00	.0	0	0	0	STAT 300
3	.000	.00	.0	0	0	0	PLOT
4	.441	-9.98	.0	70	9	0	COMP 300
5	.000	.00	.0	0	0	0	DFIT 1
6	.456	-11.23	.0	68	5	0	
8	.000	.00	.0	0	0	0	
9	.000	.00	.0	0	0	0	
COMP	.435	-10.76	.0	79	18	0	

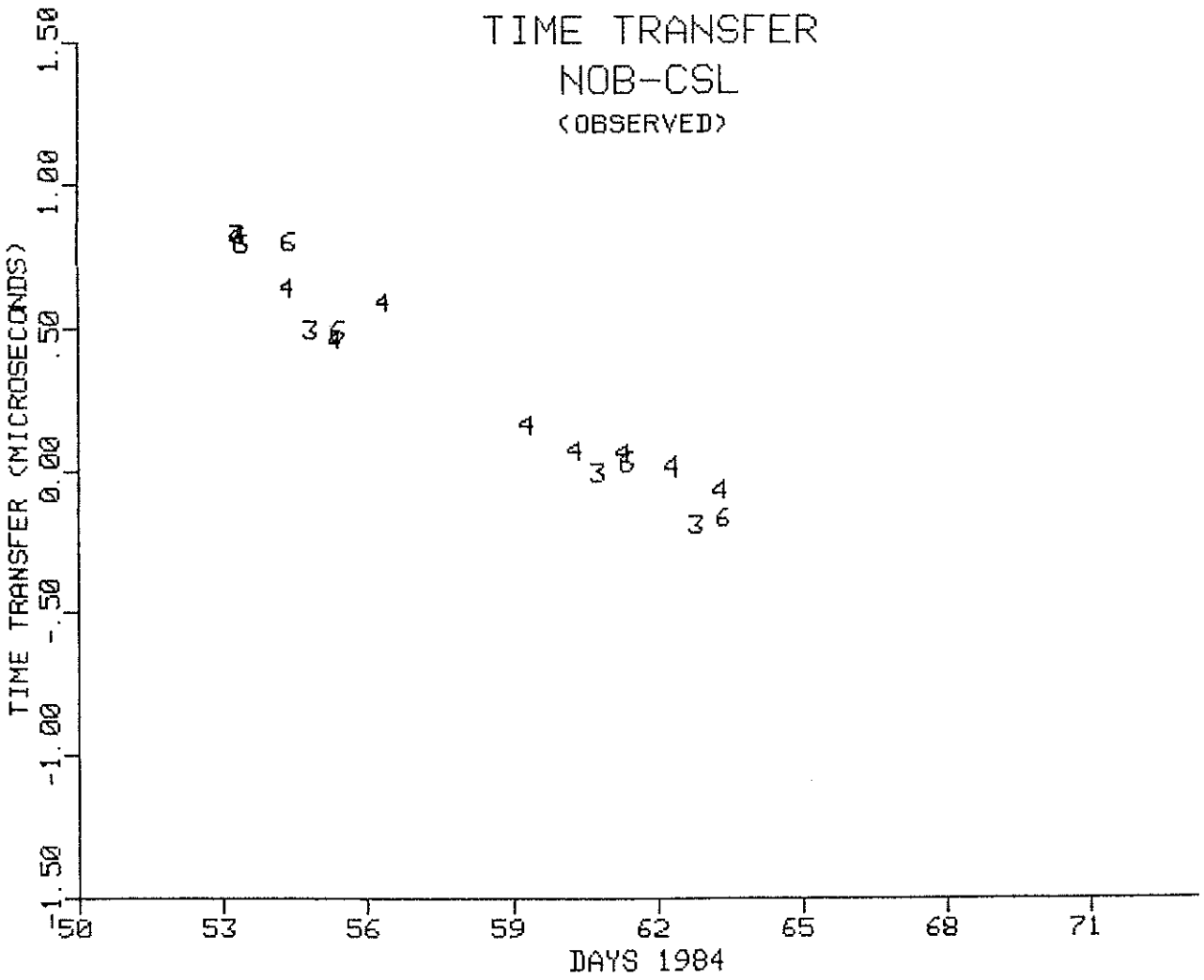

Fig. 30 NAVSTAR GPS Time Transfer

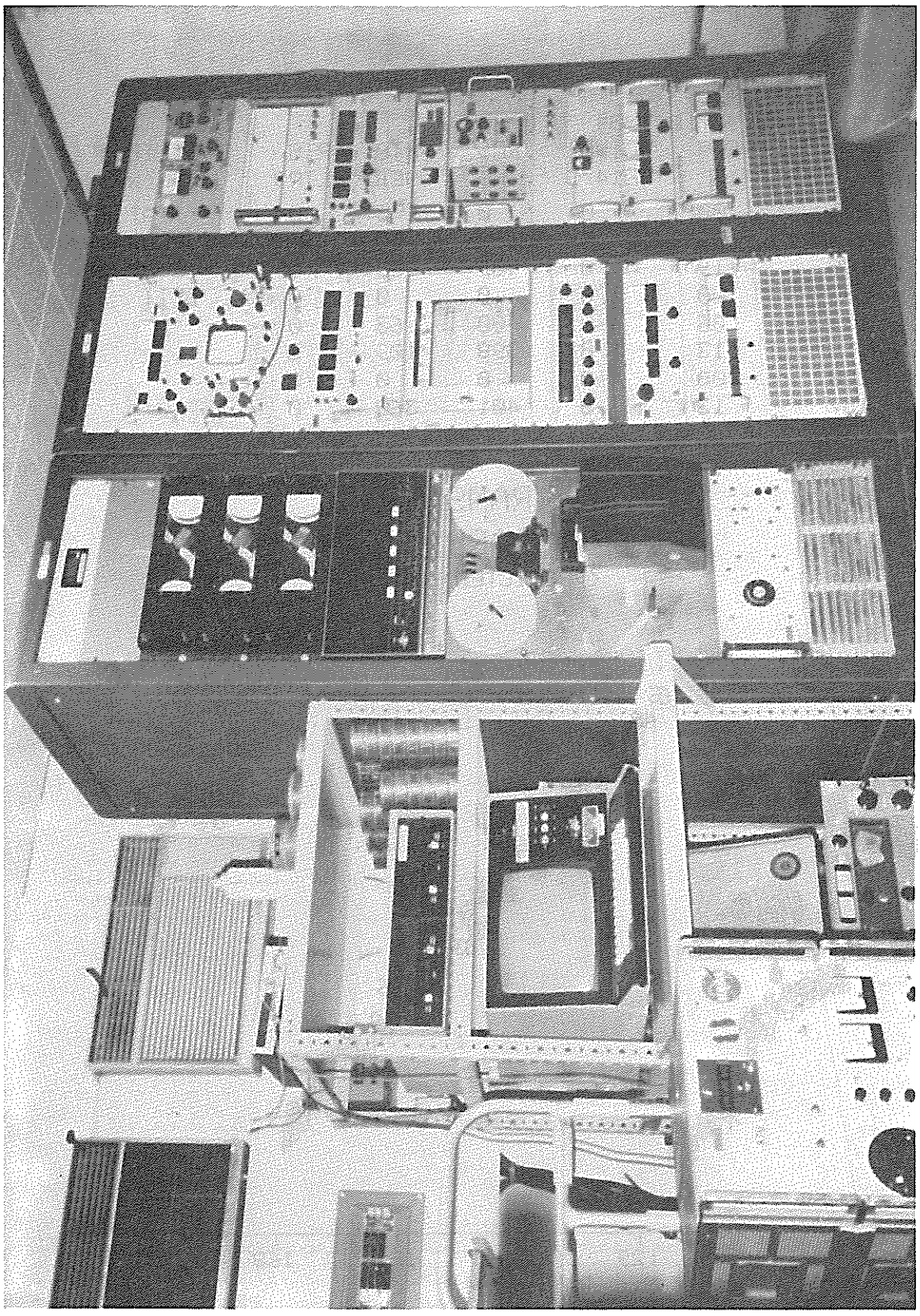

Figure 31 Arequipa, Peru Station Timing Equipment.

NAVSTAR GPS TIME TRANSFER

EPOCH DAY 137.0, 1984

SAT ID	TT US	FREQ PP13	AGING PP14/D	RMS NS	PTS USED	PTS FLTRD	FILTER TOL(NS)
1	.000	.00	.0	0	0	0	STAT 300
3	-.174	.07	.0	382	53	0	PLOT
4	-.159	.19	.0	409	135	0	COMP 300
5	.000	.00	.0	0	0	0	DFIT 1
6	-.139	.06	.0	400	63	0	
8	-.158	.13	.0	398	109	0	
9	.000	.00	.0	0	0	0	
COMP	-.157	.13	.0	401	360	0	

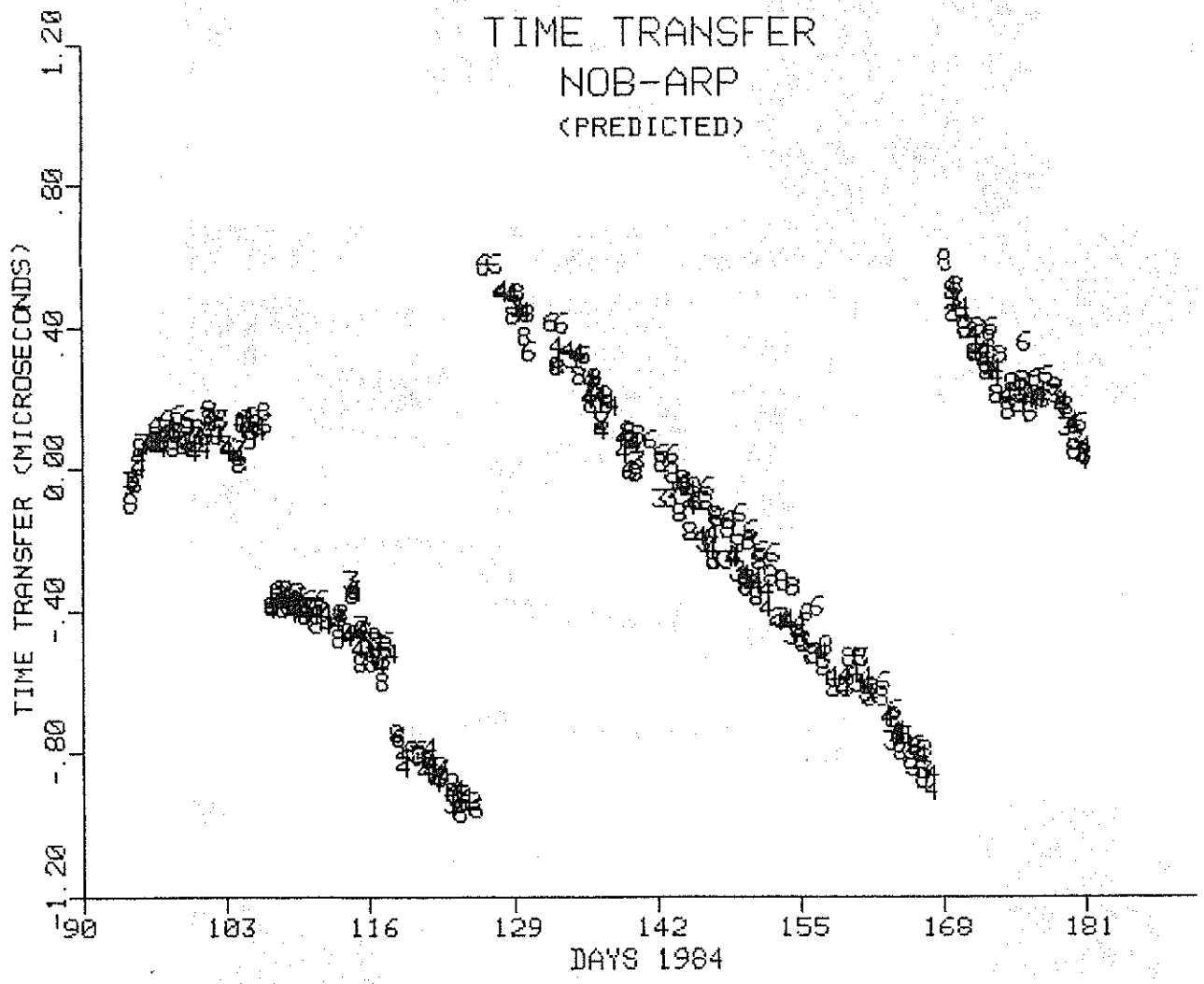

Fig. 32 NAVSTAR GPS Time Transfer

NAVSTAR GPS TIME TRANSFER

EPOCH DAY 137.0, 1984

SAT ID	TT US	FREQ PP13	AGING PP14/D	RMS NS	PTS USED	PTS FLTRD	FILTER TOL(NS)
1	.000	.00	.0	0	0	0	STAT 300
3	-.284	.59	.0	367	50	0	PLOT
4	-.279	.61	.0	382	65	0	COMP 300
5	.000	.00	.0	0	0	0	DFIT 1
6	-.228	.67	.0	377	59	0	
8	-.319	.58	.0	363	66	0	
9	.000	.00	.0	0	0	0	
COMP	-.279	.60	.0	374	240	0	

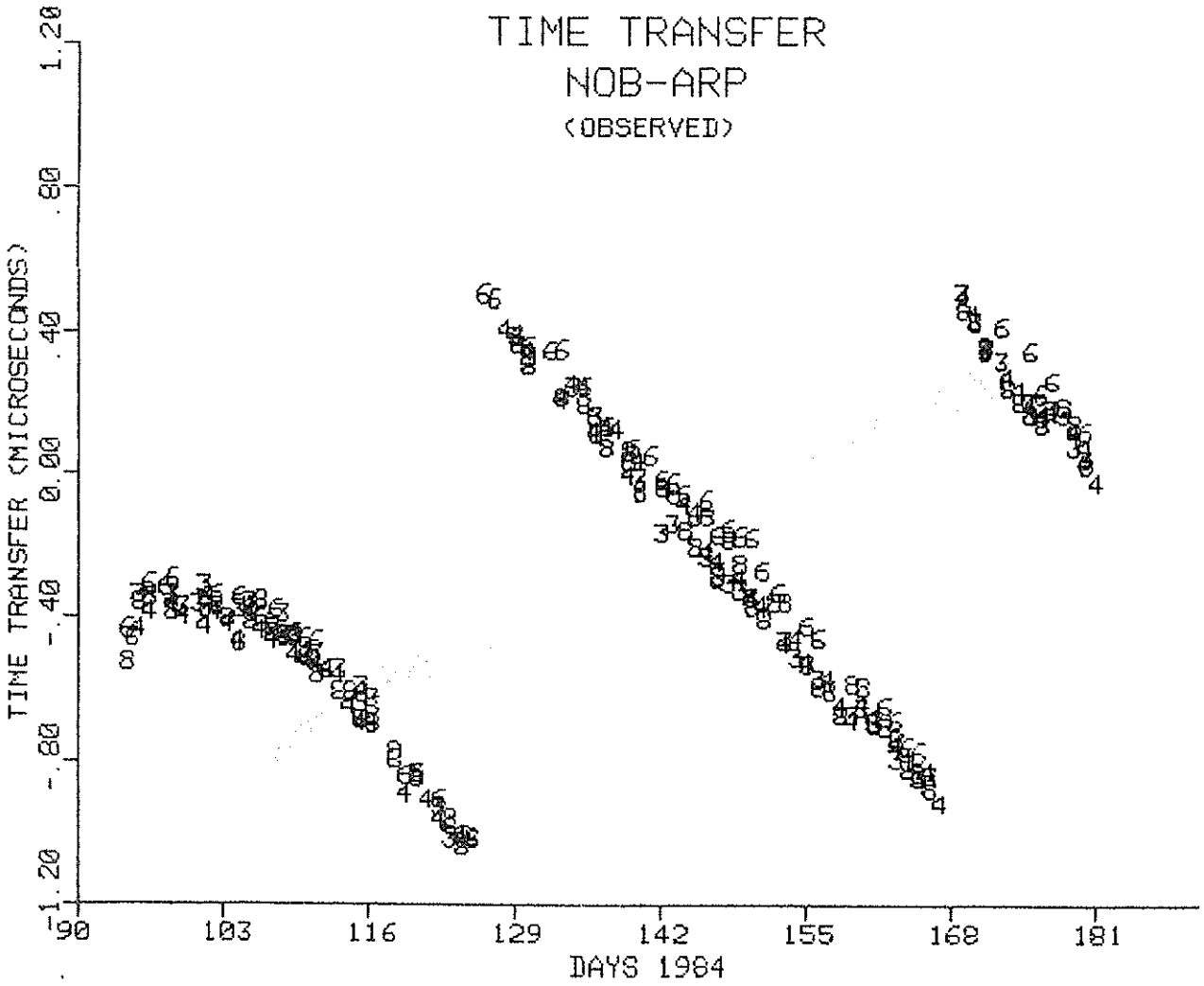

Fig. 33 NAVSTAR GPS Time Transfer

NAVSTAR GPS TIME TRANSFER

EPOCH DAY 146.0, 1984

SAT ID	TT US	FREQ PP13	AGING PP14/D	RMS NS	PTS USED	PTS FLTRD
1	.000	.00	.0	0	0	0
3	-.154	-4.06	.0	32	21	0
4	-.126	-4.09	.0	34	56	0
5	.000	.00	.0	0	0	0
6	-.069	-3.84	.0	50	30	0
8	-.118	-3.96	.0	50	48	0
9	.000	.00	.0	0	0	0
COMP	-.116	-4.03	.0	51	155	0

FILTER TOL(NS)
STAT 300
PLOT
COMP 300
DFIT 1

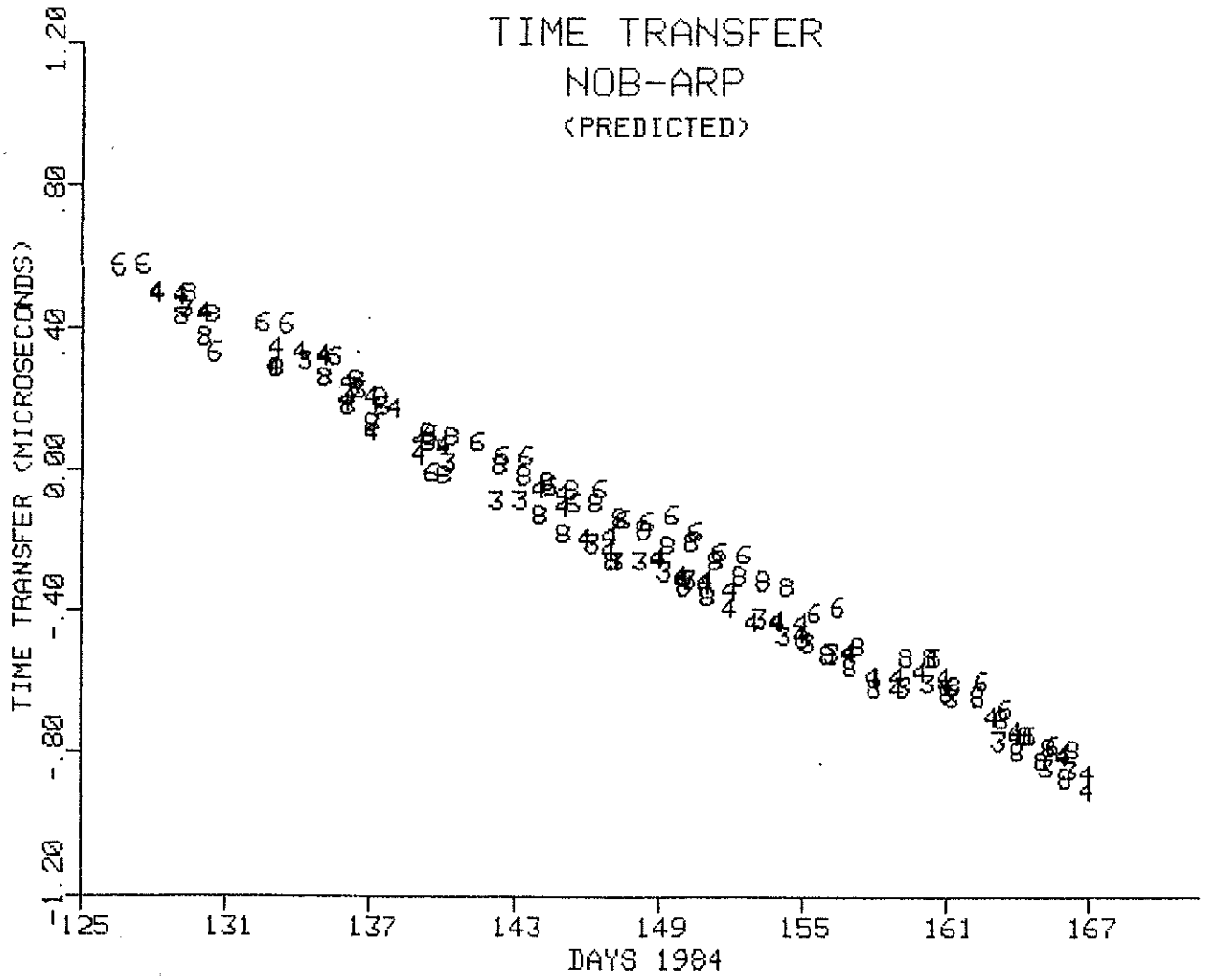

Fig. 34 NAVSTAR GPS Time Transfer

NAVSTAR GPS TIME TRANSFER

EPOCH DAY 146.0, 1984

SAT ID	TT US	FREQ PP13	AGING PP14/D	RMS NS	PTS USED	PTS FLTRD	FILTER TOL(NS)
1	.000	.00	.0	0	0	0	STAT 300
3	-.206	-3.91	.0	31	22	0	PLOT
4	-.179	-3.95	.0	32	29	0	COMP 300
5	.000	.00	.0	0	0	0	DFIT 1
6	-.114	-3.78	.0	32	28	0	
8	-.184	-3.83	.0	43	32	0	
9	.000	.00	.0	0	0	0	
COMP	-.169	-3.92	.0	49	111	0	

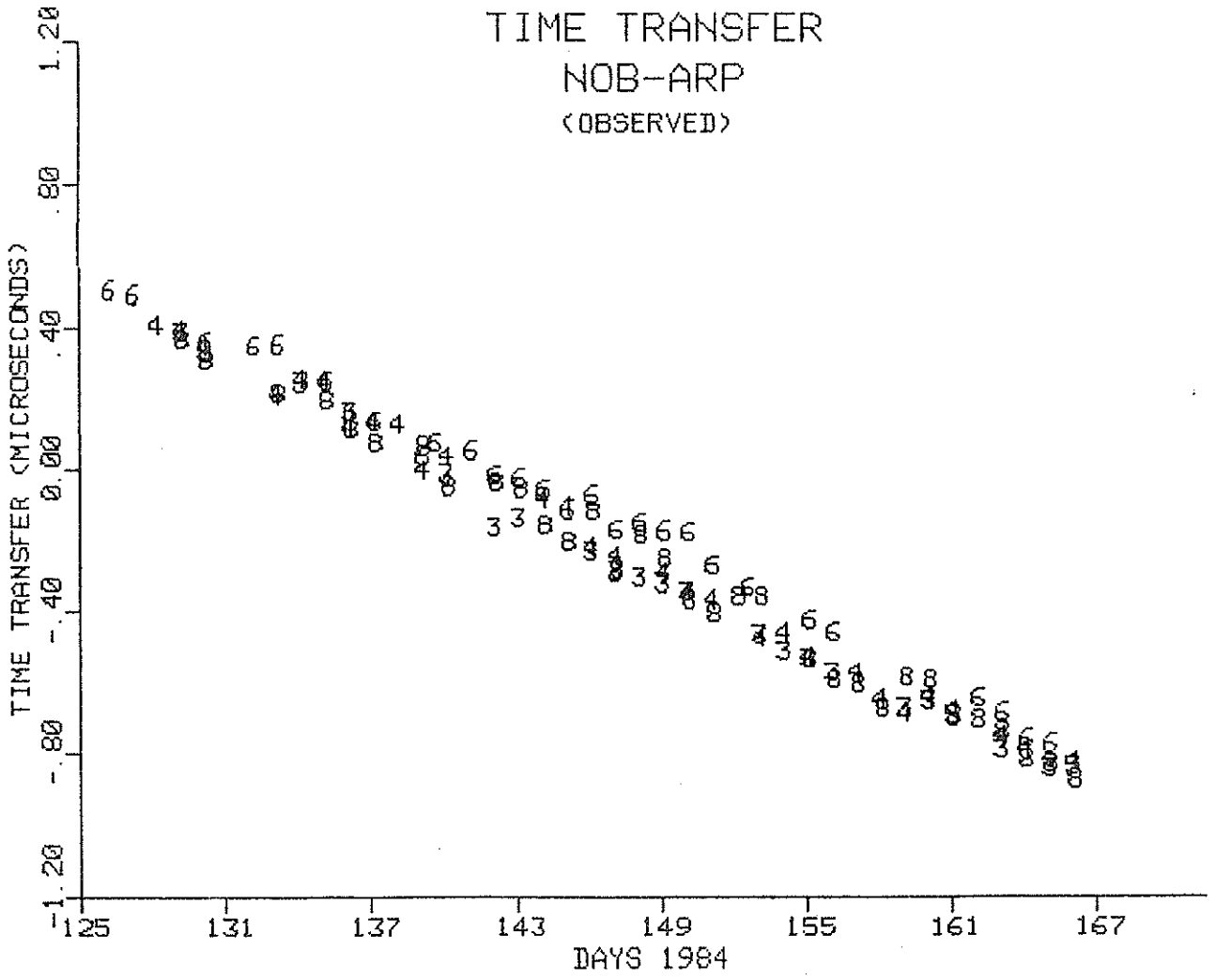

Fig. 35 NAVSTAR GPS Time Transfer

NAVSTAR GPS TIME TRANSFER

EPOCH DAY 158.0, 1984

SAT ID	TT US	FREQ PP13	AGING PP14/D	RMS NS	PTS USED	PTS FLTRD	FILTER TOL(NS)
1	.000	.00	.0	0	0	0	STAT 300
3	17.053	201.92	82.0	19	7	0	PLOT
4	17.049	201.12	81.5	35	6	0	COMP 300
5	.000	.00	.0	0	0	0	DFIT 2
6	17.064	202.30	81.3	78	12	0	
8	.000	.00	.0	0	0	0	
9	.000	.00	.0	0	0	0	
COMP	17.063	201.88	80.4	62	25	0	

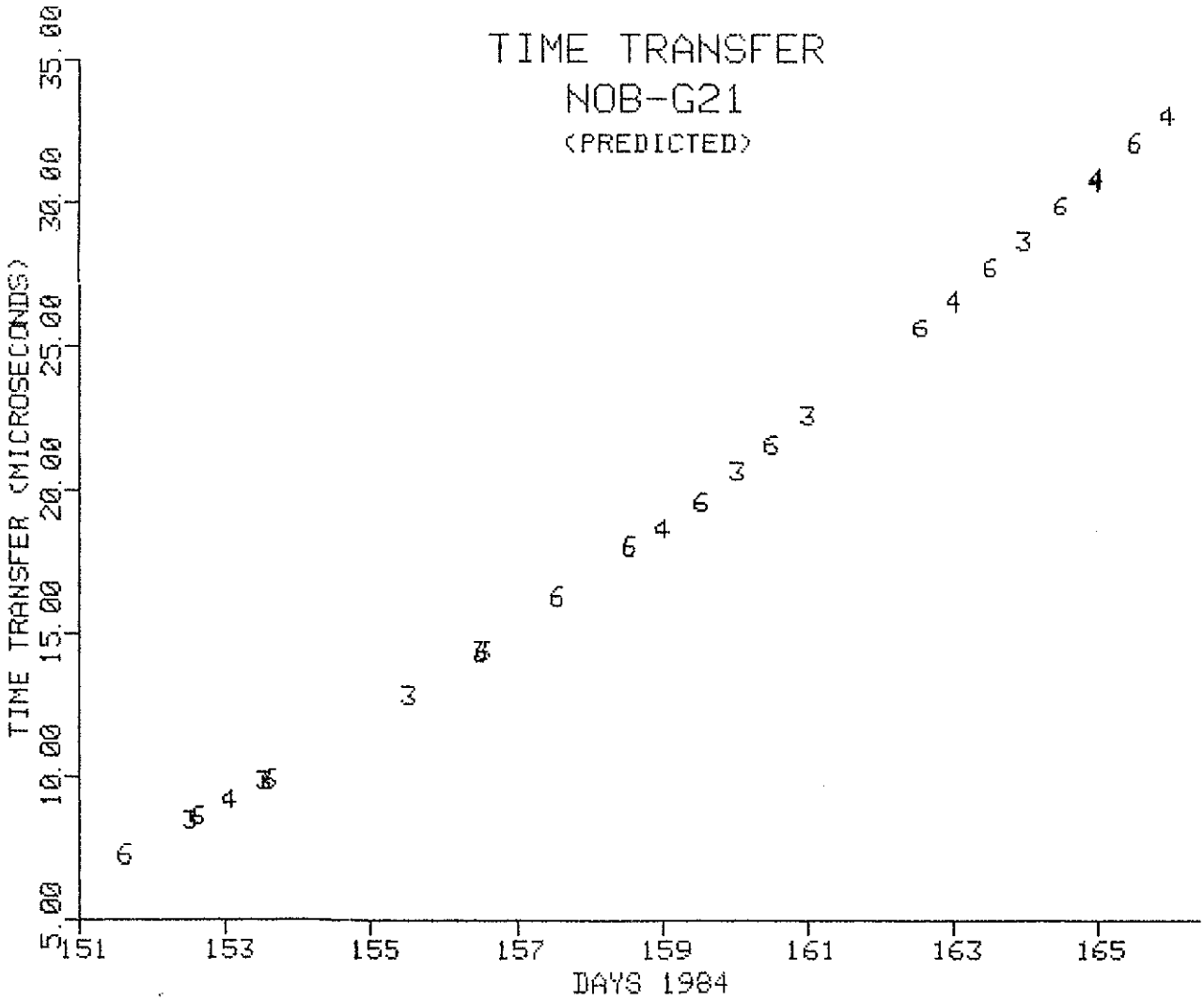

Fig. 36 NAVSTAR GPS Time Transfer

A FIBRE OPTIC TIME AND FREQUENCY DISTRIBUTION SYSTEM

D. Kirchner, H. Ressler
Institut für Nachrichtentechnik
und Wellenausbreitung
Technische Universität Graz
Inffeldgasse 12 A-8010 Graz

Telephone (0) 316 7061 ext. 7441
Telex 31221

ABSTRACT

A fibre optic time and frequency transfer system is described which is used at the Observatory Lustbühel Graz for the distribution of one pulse per second and a 10 MHz reference frequency. In developing this system special emphasis was laid on stable distribution of frequency and timing signals (good short and long term stability).

A FIBRE OPTIC TIME AND FREQUENCY DISTRIBUTION SYSTEM

INTRODUCTION

For many applications it is necessary to distribute standard frequencies and/or timing signals inside a building or between buildings. In such applications problems may arise due to ground loops and noise caused by electro-magnetic interference. Fibre optic transmissions by-pass all these problems. At the time-keeping station of the Lustbühel Observatory Graz, Austria, such a system was developed.
The system should meet the following requirements:

- Stable distribution of frequency and timing signals (good short- and long-term stability)
- Suitable for distances up to several hundred metres (adaptable to greater distances if necessary)
- Built as modular system
- Compatible with existing devices (TTL compatible signal levels, 50 ohms termination)
- Built of components available off the shelf
- High reliability
- Low price

The performance of the system should be comparable to commercially available devices in conventional technique as widely used in time-keeping laboratories.

BLOCK DIAGRAM

Fig. 1 shows the block diagrams of the frequency and the time distribution link. Although in principle it is possible to distribute both kinds of signals by the same link it is favourable to use two different links (each best suited for one of the tasks) because of the possible different duty cycles of the timing signals.
The following functional blocks are common to both systems:

- Input circuits with adjustable trigger levels
- Optic transmitter with adjustable driving current and optic receiver
- Fibre optic cable and connectors
- AC-coupled broadband amplifier with adjustable gain
- Pulse shaping circuits and line drivers

The time distribution link contains additional circuitry in the transmitter and receiver in order to be able to distribute signals of different duty cycles without changes of the throughput delay and to produce an output pulse of equal length irrespective of the input signal. In order to accommodate the link to different distances and to compensate for variations in the optic components the driving current of the optic transmitter and the gain of the amplifier in the receiver can be adjusted.

FIBRE OPTIC SYSTEM COMPONENTS

The requirements given in the introduction led to the following choice:

- Wave length: 820 nm

- Transmitter: LED with a rise time of about 10 ns and an optic output power between 5 and 25 µW at 820 nm
- Receiver: PIN-photodiode with integrated low noise transimpedance preamplifier and an output rise time of about 14 ns
- Cables: Multimode glass fibre cables (stepped index and partially graded index cables with core diameters of 200 and 100 µm, attenuation of 5 to 10 dB/km and a dispersion (pulse spreading) of about 18 ns/km
- Connectors: Factory and user installed connectors with typical insertion losses of 1.5 dB.

An important aspect for the choice of the components was the compatibility of the products of different manufacturers.

CIRCUIT DESIGN

Because of the rise times of the optic components (more than 10 ns) and in order to be compatible with widely used equipment TTL technique is used. To achieve the required low jitter values a carefully design of the print circuit boards was necessary. Besides usual filtering of the supply voltages the supply for critical components is filtered individually and the prints are designed like RF-prints (one side massive ground) to get short connections to ground (see Fig. 2). For the negative supply voltages needed for the operational amplifiers and comparators voltage inverters are used so that only positive supply voltages (5 V and 13 V) are needed. The input impedance is 50 ohms and the output signals are provided by fast line drivers delivering TTL levels into 50 ohms terminations with rise times of about 5 ns.

MAINFRAME

In order to achieve the greatest possible flexibility the device is of modular construction. The mainframe which is rack mountable (standard 19 inch rack) or for desk-top use contains the power supply (line voltage and/or 24 V DC with automatic switch-over in case of a power failure) and has space for 11 plug-ins. All available plug-ins (fibre optic transmitter and receiver for frequency and timing signals, distribution amplifiers and frequency dividers) fit in any slot of the mainframe. At the front panel signals are available which indicate if a slot is occupied and if a signal is supplied to a plug-in (front and rear panel design can be seen from Fig. 3).

PERFORMANCE

Fig. 4 shows the relation between signal jitter (standard deviation of 100 measurements of the output signal referred to the input signal), LED driving current and the length of the fibre optic link. The measurement points are for cable lengths of 10 and 100 m and driving currents of 20 and 40 mA. With the presently used optic transmitters a jitter of less than 50 ps can be achieved for distances up to several hundred metres. It is easily possible to increase the distance by the use of high efficiency fibre optic transmitters. Temperature induced changes of the throughput delay of the optic transmitter and receiver are below 30 and 50 ps/°C, respectively. Temperature induced changes of the cable delay depend on the design of the

cable used (about 5 to 17 ps/°C for a cable of 100 m length). Measurements of the signal delays on a 100 m link carried out in an air-conditioned room over a period of about one month showed no systematic changes. For several month the link is used to transmit time and frequency from the time-keeping station to the laser station of the Observatory Lustbühel and works without any problems (see the report of G. Kirchner, this issue).

ACKNOWLEDGEMENTS

The work was made possible by grants of the Austrian Council for Scientific Research and the Austrian Academy of Sciences.

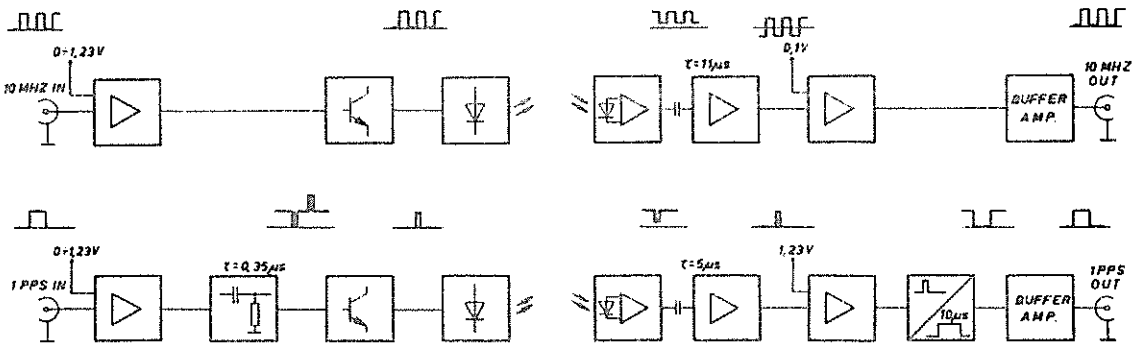

Fig. 1 Block Diagrams of the Frequency and Time Distribution Links

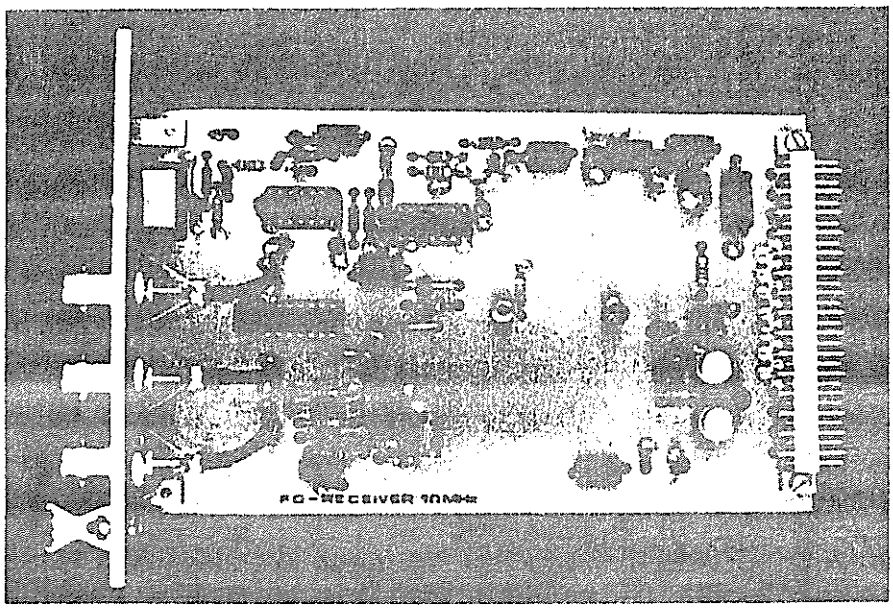

Fig. 2 Fibre Optic Plug-in (Receiver for 10 MHz)

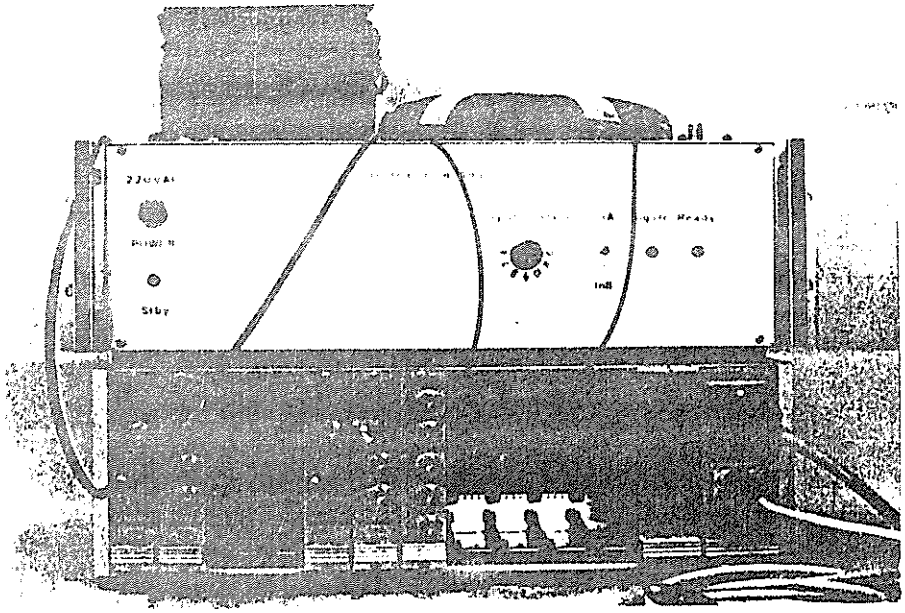

Fig. 3 Mainframe (Front and Rear Panel)

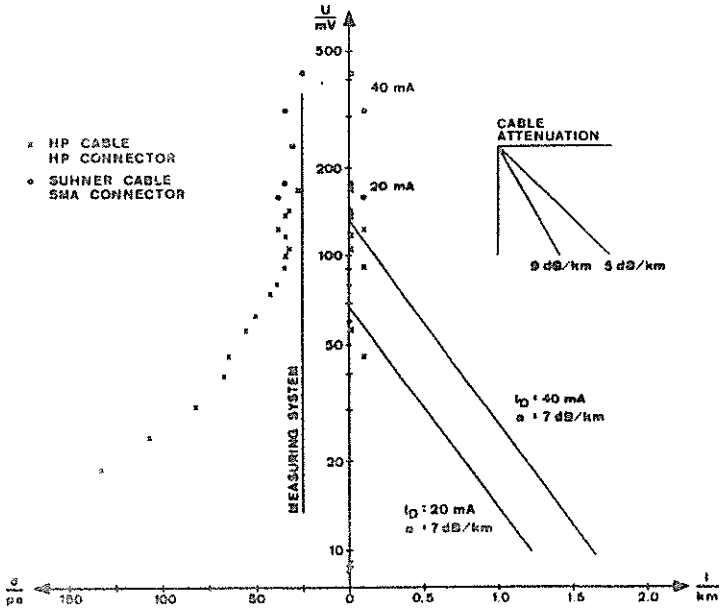

Fig. 4 Signal Jitter as aFunction of LED Driving Current, Link Length and Cable Attenuation

RECENT IMPROVEMENTS IN DATA QUALITY FROM MOBILE LASER SATELLITE TRACKING STATIONS

D.R. Edge, J.M. Heinick
Bendix Field Engineering Corporation
Data Services Group, Greenbelt, MD 20771

Telephone (301) 964 7000
Telex 197700

ABSTRACT

Since 1981 NASA's Crustal Dynamics Project has been upgrading their mobile satellite laser tracking systems (MOBLAS) to improve performance. The major hardware modifications include the installation of a short pulse high energy Quantel laser, operating at 5 hertz, with a supporting time interval unit (TIU) and a quad integrator receive energy measurement device. Calibration stability and precision as well as satellite data precision have been improved by these changes based on recent results from MOBLAS stations located in the U.S and in Australia. Full deployment of these stations will significantly improve the accuracy of the global laser data set which will lead to the more accurate determination of geophysical parameters.

Recent Improvements in Data Quality from Mobile Laser Satellite Tracking Stations

Since 1981 NASA's Crustal Dynamics Project has been upgrading their mobile satellite laser tracking systems (MOBLAS) to improve performance. The major hardware modifications include the installation of a short pulse high energy Quantel laser, operating at 5 hertz, with a supporting time interval unit (TIU) and a quad integrator receive energy measurement device. Calibration stability and precision as well as satellite data precision have been improved by these changes based on recent results from MOBLAS stations located in the U.S. and in Australia.

Full deployment of these stations will significantly improve the accuracy of the global laser data set which will lead to the more accurate determination of geophysical parameters.

Since 1981 NASA's Crustal Dynamics Project has been upgrading their mobile laser satellite tracking systems, usually referred to as MOBLAS stations. The major hardware modifications, shown to the right in Figure 1, include a new laser, time interval unit, and receive energy measurement unit. General Photonics lasers, with a pulse width of about 6 nanoseconds, are being replaced by high energy, short pulse, Quantel lasers which have a pulse width of only 2 tenths of a nanosecond. At the same time Hewlett-Packard 5370A Time Interval Units are replacing the HP5360's. The data from the HP5360's have a granularity of 100 picoseconds, or 1.5 cm in range, where as the HP5370's have a resolution of 20 picoseconds. Nonlinear Relative Energy Measurement modules measuring receive energy are being replaced with quad integrators which have a more linear scale. Also, the upgraded stations are tracking at five pps, occasionally resulting in LAGEOS passes having over ten thousand observations.

By the end of this year all but 2 of the current MOBLAS stations will have been upgraded, as shown in Figure 2. MOBLAS 1 is currently being scheduled for upgrade, while MOBLAS 2 will stop tracking and be dismantled. MOBLAS 3 is undergoing a major upgrade involving the replacement of the on-site computer in addition to the other modifications and should be back up sometime this year. The upgrades are complete on MOBLAS stations 4, 5 and 7; the upgrade with the installation of an HP5370 time interval unit later this year.

Installation of short pulse lasers greatly improved the quality of the data. In general, the calibration precision has improved by a factor of five, precalibration to postcalibration shifts have been dramatically reduced from a few tenths of nanoseconds to a few hundredths of nanoseconds, and RMS values for LAGEOS passes dropped from a range of 10 to 16 cm to the 2 to 4 cm range. This improvement in LAGEOS data can be seen in data from MOBLAS 4 in the United States and from MOBLAS 5 in Australia. Figures 3 and 4 list several LAGEOS passes taken before, and then after, the upgrades. The RMS values are plotted to the right, using the letter 'C' for combined pre- and post- calibration, and the letter 'S' for LAGEOS data. The vertical, dotted lines are at 2 centimeter intervals. At MOBLAS 4 before the upgrades, calibration RMS values were typically about 6 cm, and LAGEOS data were about 12 cm RMS. After the upgrades, calibration RMS values were down around 2.25 cm, while LAGEOS data had RMS values of about 4 cm. The improvement in the data from MOBLAS 5 was even more dramatic. Calibration RMS values went from about 5.5 cm down to 1 cm, and LAGEOS RMS values which were around 14 cm fell down to the 2 cm level.

With this large improvement in data quality it is now possible to see systematic effects at the subcentimeter level. The systematic effect from the upgraded MOBLAS stations which has received the most attention is the dependence of the range measurement on receive energy. The quad integrator allows accurate monitoring and modeling of the receive energy dependent bias and jitter of the receivers which have not yet been modified. Figure 5 is a plot of satellite data residuals versus the receive energy measurement and a plot of the receive energy distribution. The means of the range residuals in each column of the plot are plotted vertically, in centimeters, using 'X's' with one sigma error bars. The number of data points represented by each column is read downward at the bottom of the chart. The relative receive energy increases to the right. This data is from a LAGEOS pass which has an overall RMS of 2.8 centimeters, taken August 17 of this year by MOBLAS 7. As the receive energy approaches the threshold of the receive system, to the left in the plot, the delay of the system usually increases, and range measurements taken near threshold would appear to be long by a few centimeters. Also, system jitter is greater in this area, so pass RMS values increase as more data is taken near threshold. At present a large fraction of the LAGEOS data being taken by the upgraded MOBLAS systems have receive energies near the threshold limit, so it is important to monitor, model, and, if possible, correct the data based on receive energy. Upgraded MOBLAS systems now take 2000 calibration observations per pass, covering the entire receive energy range. Data has been corrected, on an experimental basis, by fitting a curve through the calibration data and then applying that curve to the satellite data, removing the bias. RMS values generally improve, some by as much as 35%, depending on the magnitude of the original biases and the distribution of data near threshold. Figure 6 is an example, a 2.7 cm LAGEOS pass taken May 13, 1984 by MOBLAS 7, was corrected based on receive energies reducing the RMS to 2.3 cm and eliminating shot by shot range biases of up to several centimeters.

To sum up, a new level of data quality has been achieved by the upgraded MOBLAS systems. LAGEOS passes now have RMS values of 2 to 4 cm, and pre- to post- calibration shifts have been greatly reduced. Data quality should improve again in the near future as new types of receivers involving microchannel plates and new discriminators are to be tested this year, and new software is being developed to handle systematic effects left in the data. LAGEOS pass RMS values should approach 1 centimeter in the near future.

LASER PULSE TIMING SYSTEM

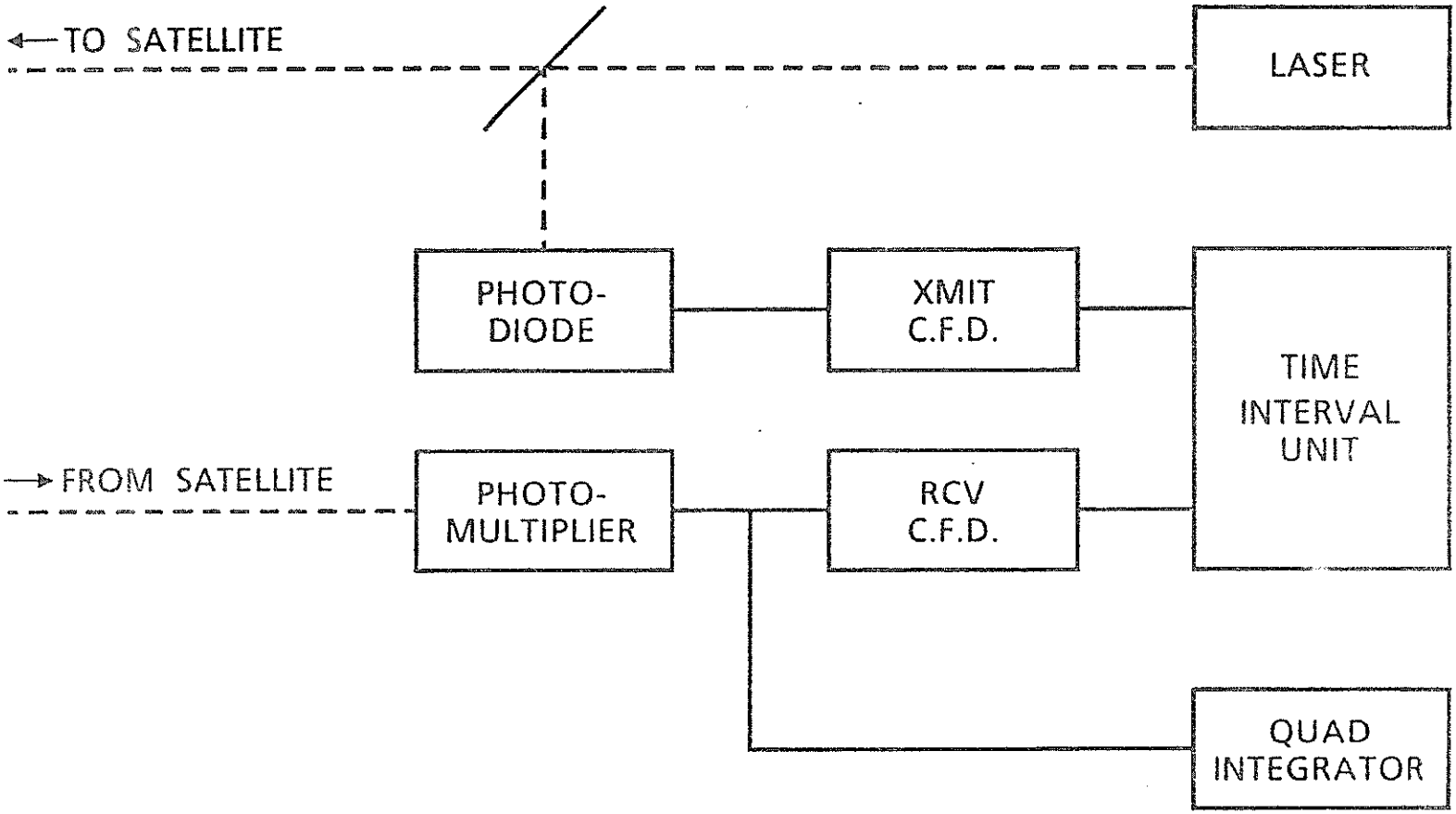

Figure 1

MOBLAS UPGRADES

STATION	LOCATION	QUANTEL LASER	HP5370 TIU	QUAD INTEGRATOR
MOBLAS 1	French Polynesia	(To be scheduled)	N/A	N/A
MOBLAS 2	Platteville, CO	(To be dismantled)	N/A	N/A
MOBLAS 3	Greenbelt, MD	1984	1984	1984
MOBLAS 4	Monument Peak, CA	1982	1982	1982
MOBLAS 5	Western Australia	1983	1983	1983
MOBLAS 6	Mexico	1984	1984	1984
MOBLAS 7	Greenbelt, MD	1983	1982	1983
MOBLAS 8	Quincy, CA	1982	(1984)	1982

Figure 2

MOBLAS 4 LAGEOS PASSES BEFORE QUANTEL

DATE	GMT		CALIBRATION ('C') AND SATELLITE ('S') RMS (CM)								
			2	4	6	8	10	12	14	16	18
9/29/82	0308	I	.	.	C.	.	.	.	S .	.	.
9/29/82	0755	I	.	.	C	.	.	.	S .	.	.
10/22/82	0328	I	.	.	C	.	.	S	.	.	.
10/23/82	0849	I	.	.	C	.	.	.S	.	.	.
10/27/82	0340	I	.	.	.	.	C .	S	.	.	.
10/28/82	0915	I	.	.	. C	.	.	.	S.	.	.
10/30/82	0306	I	.	.	.	.	.	C	S .	.	.
10/30/82	0625	I	.	. C	.	.	.	.	S .	.	.
11/03/82	0437	I	.	.	.C	. S	.	.	.	.	.
11/03/82	2349	I	.	.	.C	.	.S	.	.	.	.
11/04/82	0322	I	.	. C	.	.	.	.	.	.	S.
11/06/82	0039	I	.	. C	.	.	.	S	.	.	.

MOBLAS 4 LAGEOS PASSES BEFORE QUANTEL

DATE	GMT		CALIBRATION ('C') AND SATELLITE ('S') RMS (CM)								
			2	4	6	8	10	12	14	16	18
5/31/83	0152	I	. C	.S	.	.	.	.	.	.	.
6/02/83	1444	I	.C	S	.	.	.	.	.	.	.
6/10/83	0206	I	.C	. S	.	.	.	.	.	.	.
6/10/83	1427	I	. C	S	.	.	.	.	.	.	.
6/14/83	0025	I	. C	S	.	.	.	.	.	.	.
6/15/83	2132	I	. C	. S	.	.	.	.	.	.	.
6/16/83	0101	I	. C	.S	.	.	.	.	.	.	.
6/16/83	2354	I	C	.S	.	.	.	.	.	.	.
6/17/83	2223	I	C	S	.	.	.	.	.	.	.
6/22/83	1557	I	. C	. S	.	.	.	.	.	.	.
6/22/83	2217	I	. C	.S	.	.	.	.	.	.	.
6/23/83	1411	I	. C	.S	.	.	.	.	.	.	.
6/23/83	2102	I	C	.S	.	.	.	.	.	.	.
6/24/83	0028	I	.	S	. C	.	.	.	.	.	.

Figure 3

MOBLAS 5 LAGEOS PASSES BEFORE QUANTEL

DATE	GMT		CALIBRATION ('C') AND SATELLITE ('S') RMS (CM) 2 4 6 8 10 12 14 16 18
3/28/83	1446	I	C S
3/28/83	1817	I	C S
3/30/83	1910	I	C S
4/10/83	1448	I	C S
4/10/83	1812	I	C S
4/11/83	1648	I	C S
4/13/83	1403	I	C S
4/13/83	1738	I	C S
4/17/83	1541	I	C S
4/18/83	1754	I	C S
4/19/83	1259	I	C S
4/19/83	1628	I	C S
4/21/83	1720	I	C S
4/25/83	1856	I	C S
4/26/83	1356	I	C S

MOBLAS 5 LAGEOS PASSES BEFORE QUANTEL

DATE	GMT		CALIBRATION ('C') AND SATELLITE ('S') RMS (CM) 2 4 6 8 10 12 14 16 18
11/01/83	1341	I	C S
11/01/83	1645	I	C S
11/02/83	1517	I	C S
11/03/83	1404	I	C S
11/07/83	1532	I	C S
11/08/83	1414	I	C S
11/08/83	1741	I	C S
11/09/83	1304	I	C S
11/09/83	1615	I	C S
11/10/83	1500	I	C S
11/10/83	1830	I	C S
11/21/83	1734	I	C S
11/22/83	1254	I	C S
11/22/83	1609	I	C S
11/23/83	1449	I	C S

Figure 4

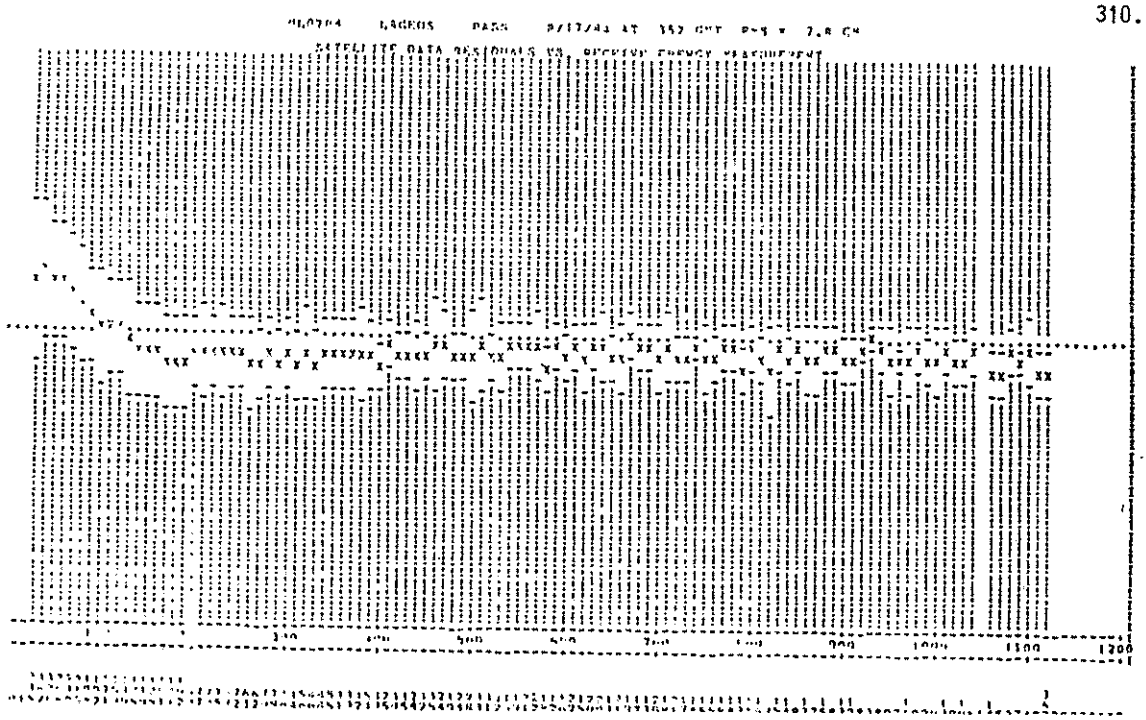

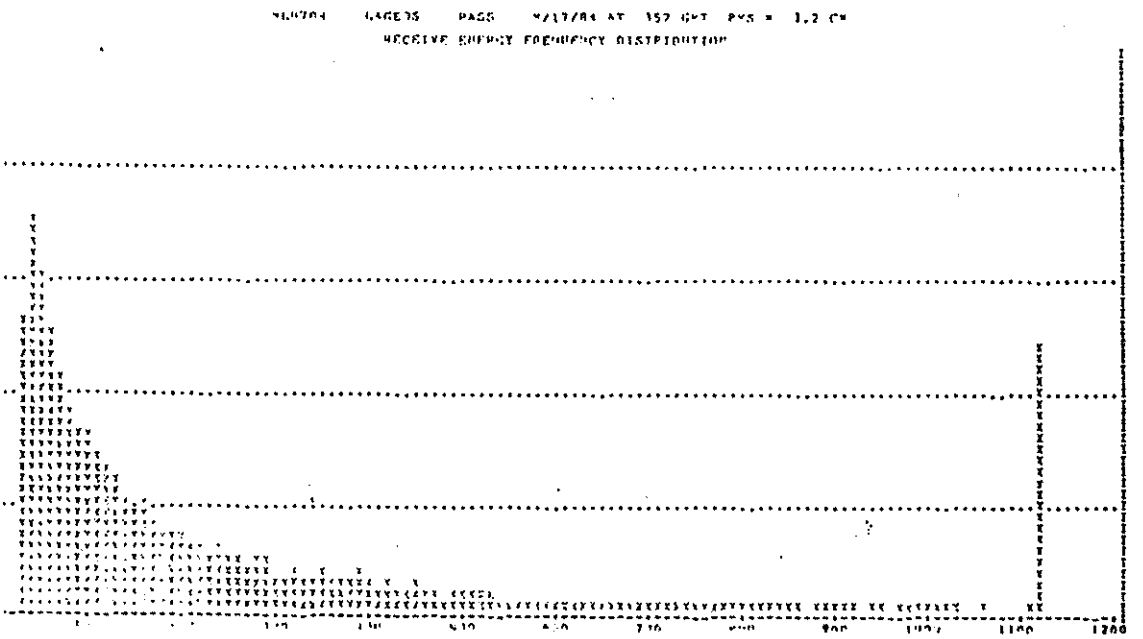

Figure 5

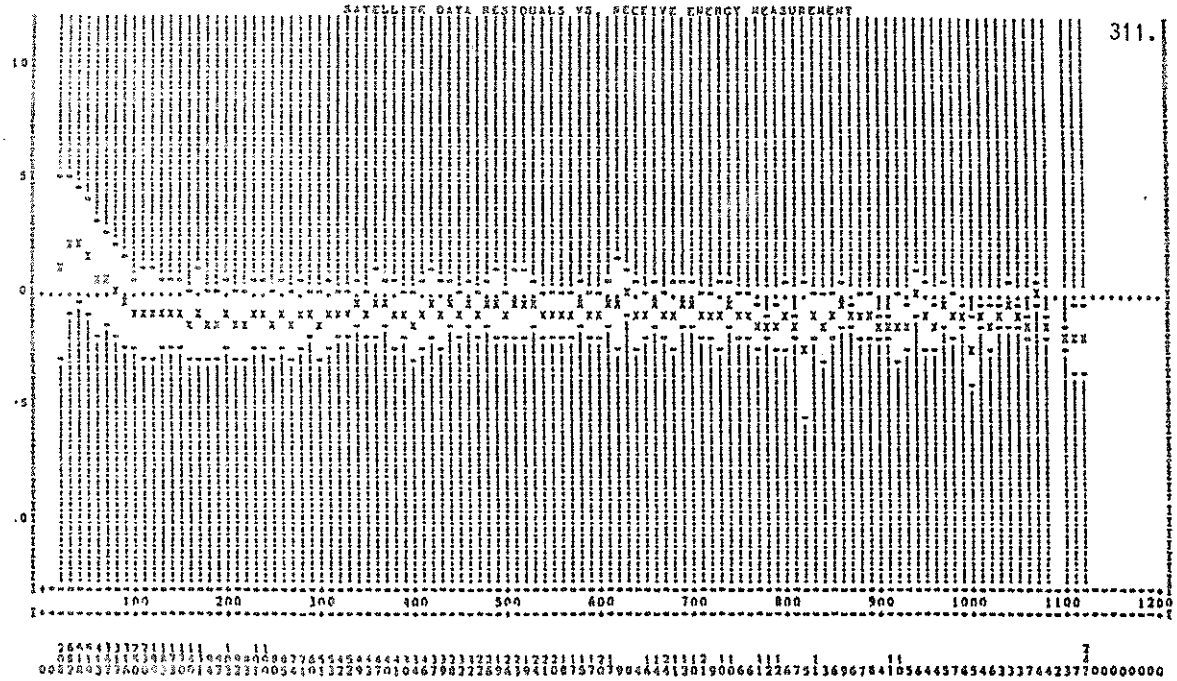
SATELLITE DATA RESIDUALS VS. RECEIVE ENERGY MEASUREMENT
100
200
300
400
500
600
700
800
900
1000
1100
1200

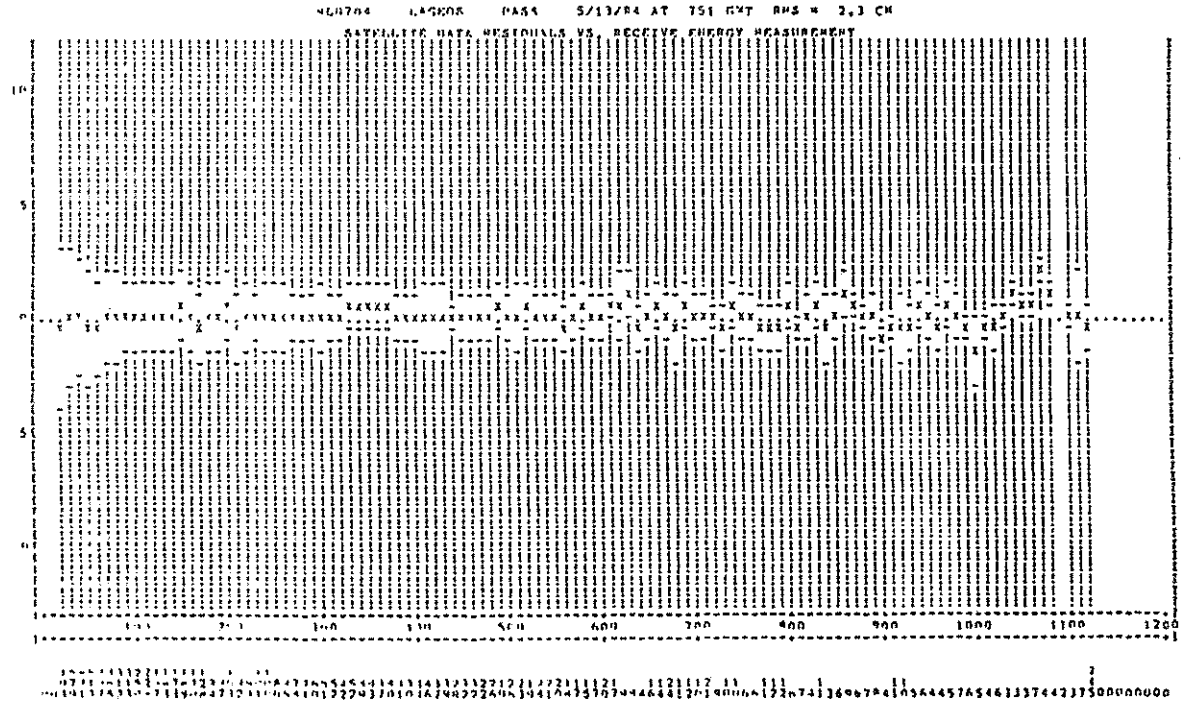
NG0704 LAGEOS PASS 5/13/84 AT 751 GMT RMS = 2.3 CM
SATELLITE DATA RESIDUALS VS. RECEIVE ENERGY MEASUREMENT
100
200
300
400
500
600
700
800
900
1000
1100
1200

Figure 6

CURRENT MOBLAS DATA QUALITY CONCLUSIONS

* LAGEOS PASS RMS VALUES HAVE BEEN REDUCED TO THE 2 TO 4 CM LEVEL.
* CALIBRATION STABILITY HAS BEEN GREATLY IMPROVED.
* CALIBRATION PRECISION HAS IMPROVED BY A FACTOR OF FIVE.
* RECEIVE SYSTEM HARDWARE DEVELOPMENT AND NEW DATA PROCESSING SOFTWARE MODELS CAN POTENTIALLY CORRECT SUBCENTIMETER SYSTEMATIC EFFECTS.
* LAGEOS PASS RMS VALUES WILL APPROACH ONE CENTIMETER IN THE NEAR FUTURE.

Figure 7